

# Open Research Online

---

The Open University's repository of research publications and other research outputs

## The “Mera” lahar deposit in the upper Amazon basin: Transformation of a late Pleistocene collapse at Huisla volcano, central Ecuador

### Journal Item

How to cite:

Bedón, Pedro Alejandro Espín; Mothes, Patricia A.; Hall, Minard L.; Arcos, Viviana Valverde and Keen, Hayley (2018). The “Mera” lahar deposit in the upper Amazon basin: Transformation of a late Pleistocene collapse at Huisla volcano, central Ecuador. *Journal of Volcanology and Geothermal Research* (Early Access).

For guidance on citations see [FAQs](#).

© 2018 Elsevier B.V.

Version: Accepted Manuscript

Link(s) to article on publisher's website:  
<http://dx.doi.org/doi:10.1016/j.jvolgeores.2018.10.008>

---

Copyright and Moral Rights for the articles on this site are retained by the individual authors and/or other copyright owners. For more information on Open Research Online's [data policy](#) on reuse of materials please consult the policies page.

---

[oro.open.ac.uk](http://oro.open.ac.uk)

## Accepted Manuscript

The “Mera” lahar deposit in the upper Amazon basin:  
Transformation of a late Pleistocene collapse at Huisla volcano,  
central Ecuador

Pedro Alejandro Espín Bedón, Patricia A. Mothes, Minard L.  
Hall, Viviana Valverde Arcos, Hayley Keen



PII: S0377-0273(17)30584-X  
DOI: [doi:10.1016/j.jvolgeores.2018.10.008](https://doi.org/10.1016/j.jvolgeores.2018.10.008)  
Reference: VOLGEO 6463

To appear in: *Journal of Volcanology and Geothermal Research*

Received date: 26 September 2017  
Revised date: 7 September 2018  
Accepted date: 8 October 2018

Please cite this article as: Pedro Alejandro Espín Bedón, Patricia A. Mothes, Minard L. Hall, Viviana Valverde Arcos, Hayley Keen , The “Mera” lahar deposit in the upper Amazon basin: Transformation of a late Pleistocene collapse at Huisla volcano, central Ecuador. *Volgeo* (2018), doi:[10.1016/j.jvolgeores.2018.10.008](https://doi.org/10.1016/j.jvolgeores.2018.10.008)

This is a PDF file of an unedited manuscript that has been accepted for publication. As a service to our customers we are providing this early version of the manuscript. The manuscript will undergo copyediting, typesetting, and review of the resulting proof before it is published in its final form. Please note that during the production process errors may be discovered which could affect the content, and all legal disclaimers that apply to the journal pertain.

# The “Mera” lahar deposit in the upper Amazon basin: transformation of a late Pleistocene collapse at Huisla volcano, central Ecuador

Pedro Alejandro Espín Bedón<sup>1</sup>, Patricia A. Mothes<sup>1</sup>, Minard L. Hall<sup>1</sup>, Viviana Valverde Arcos<sup>1</sup>, Hayley Keen<sup>2</sup>

<sup>1</sup>Instituto Geofísico, Escuela Politécnica Nacional, Casilla 1701-2759, Quito- Ecuador

<sup>2</sup>Palaeoenvironmental Change Research Group, Environment, Earth and Ecosystems, Gass Building, The Open University, Milton Keynes, MK7 6AA, Great Britain

## The “Mera” lahar deposit in the upper Amazon basin: transformation of a late Pleistocene collapse at Huisla volcano, central Ecuador

### Abstract:

The Sub-Andean zone east of the Cordillera Real, Ecuador and out to the Amazon basin's western margin has been the depository of voluminous lahars related to volcanic activity in the Andean highlands. These lahars arrived to the Sub-Andean zone via gravitational transport through narrow river canyons and emplaced volumes surpassing several cubic kilometers over robust inundation zones. This paper discusses the origin, flow route, depositional zone, terrace formation and geomorphic significance of the most important lahar deposit yet mapped in this region, that of the Mera lahar, which likely formed from a late Pleistocene collapse of Huisla volcano, followed by impounding by temporary dams behind drainage-blocking debris avalanche deposits (DAD), then subsequent rupture of the blockage. The actual deposit of the Mera lahar has a thickness between 30 to 70 meters, is mainly comprised of DAD breccia, is matrix-supported (*c* 70%), of reddish gray color and is well-consolidated. Based on geochemical and petrographic similarities, Huisla volcano's DAD is the best candidate for the lahar's source. Huisla volcano is located some 90 km up valley of the bulk of Mera lahar's mapped deposit. Clasts of Mera lahar rocks and Huisla's DAD breccias have 57-61 wt% SiO<sub>2</sub>, corresponding to andesites of the calc-alkaline series with mean values of 1-1.5 wt% for K<sub>2</sub>O. The mapped Mera lahar deposit has an actual volume estimated in 1.2 km<sup>3</sup> compared to its original estimated volume of 5.4 km<sup>3</sup>. Cross-sectional widths of 1.5 to 4.5 km span and extend laterally beyond the actual Pastaza river channel where the lahar's deposition produced high-standing isolated surfaces that are notable local geomorphic features of the upper Sub-Andean zone. The flow modeling program

LaharFlow, employing the modern landscape as the topographic base, adequately simulates the flow route and inundation zones of the Mera lahar.

KEY WORDS: Lahar deposits; Mera, Pastaza; Huisla volcano; Huisla DAD, Pastaza river; Ecuador's Sub-Andean zone

ACCEPTED MANUSCRIPT

## 1 **1.1 Introduction:**

### 2 *1.1.1 -Lahars*

3  
4 Lahars are complex mixtures of volcanic debris and water. They can be classified as debris flows  
5 (usually >50-60% sediment volume) or hyperconcentrated flows (typically 20-60% sediment volume)  
6 (Vallance, 2000; Darnell et al, 2013, Vallance and Iverson, 2015). Primary lahars may occur  
7 infrequently at volcanoes in long repose, with lapses of hundreds or more years between eruptions.

8  
9 Such is the case at Cotopaxi volcano whose huge primary lahars were associated with the destruction  
10 and melting of the perennial glacier by incandescent pyroclastic density currents related to large  
11 eruptions every 100 to 200 years (Mothes et al., 2004). On the other hand, secondary lahars at  
12 Tungurahua volcano, 80 km downriver from Cotopaxi have been a common occurrence since 1999  
13 because of ongoing eruptive activity and subsequent remobilization of fresh volcanoclastics by  
14 precipitation on steep flanks (Mothes and Vallance, 2015). Other lahars, of a more secondary origin  
15 are those that formed from damming of water bodies by debris avalanche deposits and then  
16 subsequent rupture of these temporary dams, as is the well-documented case at Mount St. Helens in  
17 1980 (Lipman and Mullinaux, 1981; Manville, 2015). A case similar to the one described herein is  
18 that at Colima volcano, Mexico when a DAD (debris avalanche deposit) blocked a river about 18.5 ka;  
19 the temporary dam overflowed and breached and the resultant lahar flowed 130 km to the Pacific  
20 Ocean (Capra and Macias, 2002). Owing to the different repose times and styles of volcanic activity,  
21 people living around or downstream of volcanoes may not anticipate or plan for dangers represented  
22 by lahars even though in the last decade lahars have killed thousands of people worldwide (Loughlin  
23 et al., 2015). Because lahars are saturated in fluids and form a dense matrix, rock fragments of varying  
24 sizes are transported and contribute to the degree of destructiveness of this phenomenon (Pierson  
25 et al., 2014).

### 26 27 28 *1.1.2 -Potential Source Volcanoes for Lahars Emplaced in Ecuador's Sub-Andean Zone*

29  
30 The Ecuadorian volcanic arc has two main cordilleras (Eastern and Western) and both of them are  
31 characterized by frequent explosive eruptions that have generated gravitational flows whose  
32 discharge and reach have been unpredictable (Hall et al., 2008). In Ecuador there are over 40  
33 potentially active volcanoes, and many of these have yet to be adequately studied (Hall et al., 2008).  
34 At least seven volcanoes in central Ecuador that drain into the Pastaza river basin have experienced  
35 Pleistocene to Holocene-age sector collapses or important slides that transformed to lahars and  
36 flowed down the montane Pastaza river. Volcanoes located in the middle Pastaza river headwaters

37 that have produced debris avalanche deposits are: Huisla and Altar (Bustillos, 2008); Chimborazo  
38 (Bernard et al., 2008; Samaniego et al., 2012); Carihuairazo (Vásconez R. et al., 2011; Vásconez et  
39 al., 2016); Quiñuales Massif (Herrera, 2013) and Tungurahua (Hall et al., 1999; LePennec et al., 2013)  
40 (Fig. 2).

41

42 The transit of lahars borne on the flanks of steep Eastern Cordillera stratocones has been mostly  
43 confined in narrow high-gradient canyons where they remobilized important volumes of  
44 volcanoclastics which then were transported eastward to the Sub-Andean Zone and continued to the  
45 low-gradient western piedmont of the Amazon basin, far from the parent volcano. Lahars can also  
46 flow over low gradients and cover broad areas, such as the long distance lahars from Cotopaxi volcano  
47 (Mothes et al., 1998, 2004).

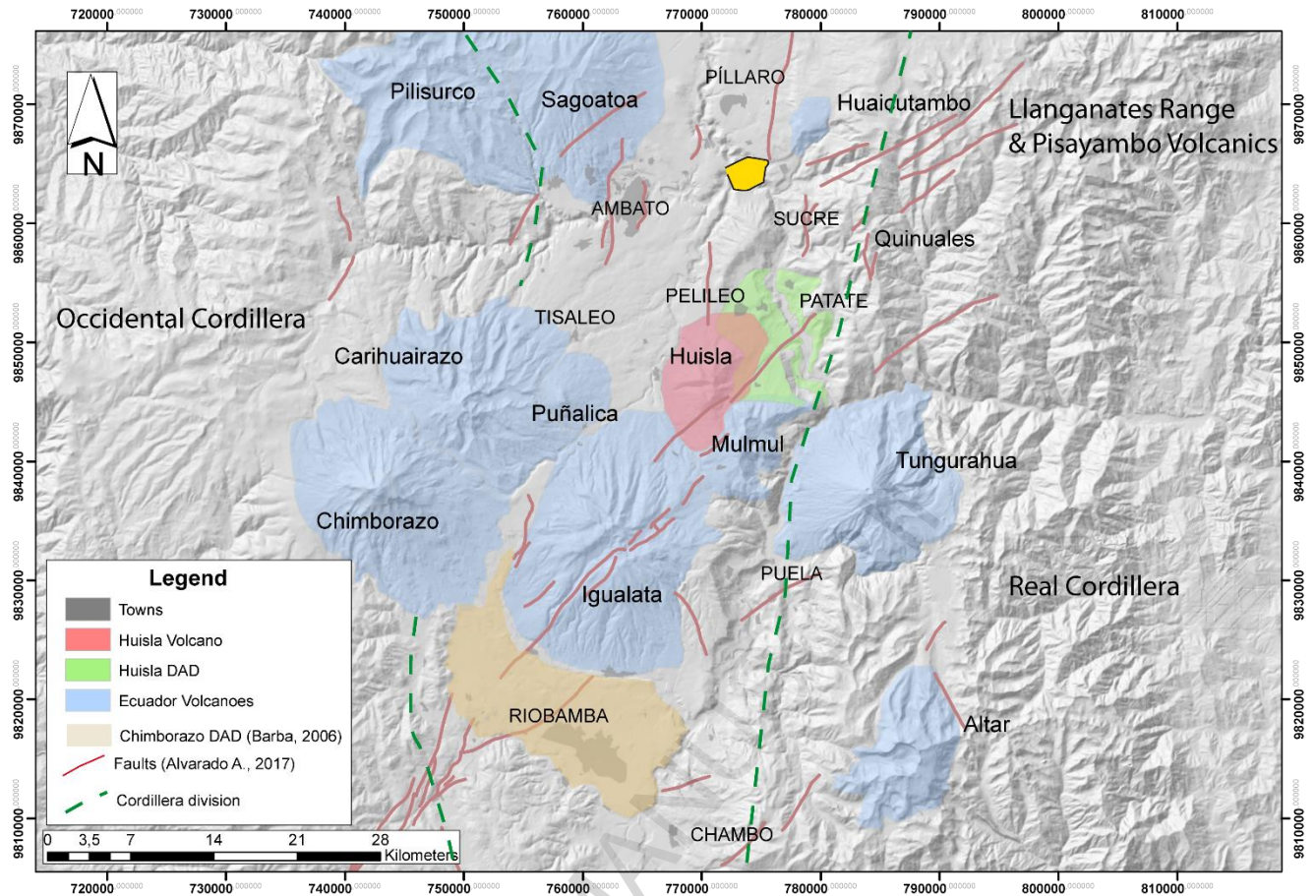
48

49

50 The aim of this contribution is to explore the origin, flow routes and landscape modification  
51 associated with the Mera lahar, whose deposits outcrop along the lower Pastaza river channel (Fig.  
52 1). The Mera lahar is an example of a large-volume flow that overtopped and extended laterally  
53 beyond the preexisting channel limits of the Rio Pastaza and left high-standing surfaces above present  
54 river level. The origin of Mera lahar is believed to be a volcanic sector collapse in the upper Pastaza  
55 river catchment and its deposit is the first to be mapped in Ecuador's Sub-Andean zone.







67  
68  
69 *Figure 2. Huisla volcano, avalanche deposit and fault trace. Yellow circle east of Ambato city represents one area of*  
70 *lacustrine deposits possibly related to the damming of the Cutuchi-Patate river system by the Huisla DAD. Chimborazo's*  
71 *DAD deposit is outlined in tan color, and is centered around the city of Riobamba, built upon the DAD.*

## 72 73 74 **2.1 Methodology**

### 75 **2.1.1 Tracing the Mera Lahar:**

76  
77  
78 In the study area we map the Mera lahar's beginnings as being emplaced into the Patate and Chambo  
79 rivers which join at "Las Juntas" to form the Pastaza River (Fig. 1 & 2). The Pastaza River is the  
80 master river in the area and has numerous second order high-gradient inflowing streams between  
81 Baños to El Topo town (Fig. 3). Between El Topo and Mera towns the Pastaza canyon verves sharply  
82 south as it cuts through granites of the Abitagua batholith, where the canyon width is approximately  
83 only 0.5 km wide and Mera lahar may have experienced resistance to flow while traversing the narrow  
84 canyon, since the lahar flowed up the side canyon of the Topo river for more than 700 meters in a SW  
85 direction.

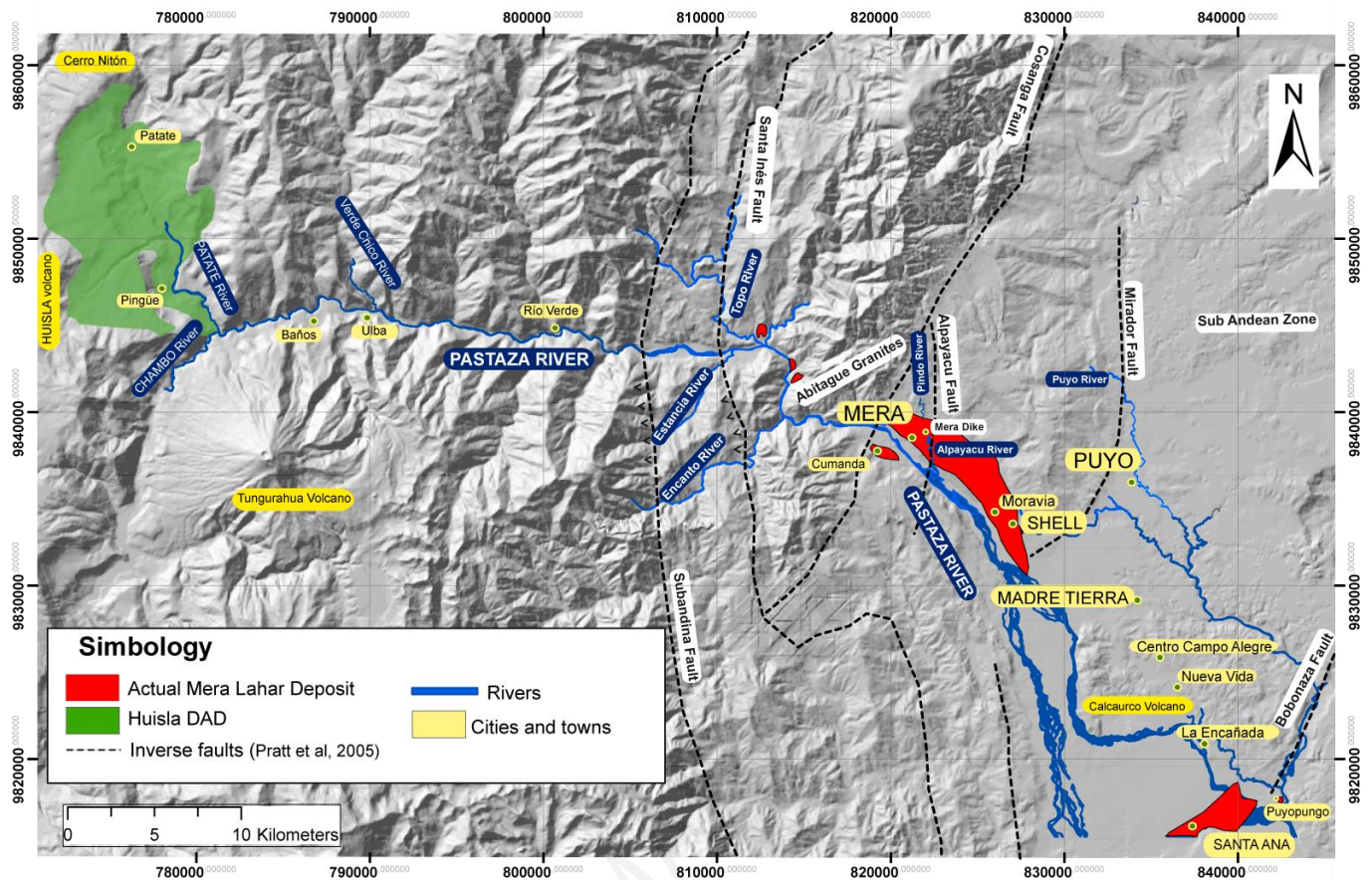
86 Flowing up side canyons due to hydraulic damming in the main channel was also a characteristic of  
87 the giant Osceola Mudflow, Rainier volcano during transit (Vallance and Scott, 1997).

88 Below Mera town the Pastaza receives inputs of the Pindo and Alpayacu rivers (Figure 1), both borne  
89 on the Abitagua massif (Pratt et al., 2005). The majority of the outcrops of the Mera lahar deposit lie  
90 between El Topo and Santa Ana on the left margin of the Pastaza River (Fig. 3), with towns of Mera  
91 and Moravia and others all built upon the terraces consisting of the lahar deposit. Along the Pastaza's  
92 right margin only one outcrop is recognized at Cumanda. Following original deposition all along the  
93 Pastaza river and reflux into incoming side channels, such as that of the Alpayacu River, subsequent  
94 lateral erosion of the deposit has left outstanding terraces upon which the mentioned towns are  
95 established on the Pastaza's left margin.

96

97 River-borne deposits overlying the Mera lahar were discharged from the local Alpayacu river  
98 descending the Abitagua massif and the deposits are mainly granitic clasts, contrasting strongly with  
99 the andesitic components of Mera lahar. Further downriver at Santa Ana younger reworked  
100 volcanoclastic layers from the Calcaurcu volcanic complex (Ball, 2015) overly the lahar deposit. We  
101 do not observe other gravitational flow products of volcanic origin overlying the present surface of  
102 the Mera lahar (Fig. 3), even though two sector collapses of Tungurahua volcano reported by Hall et  
103 al. (1999) could possibly have had sufficient flow heights along the lower Pastaza to overbank onto  
104 the Mera lahar depositional surface.

105



106  
107 *Figure 3. Mera lahar deposit map based on field mapping. Fault traces modified from Pratt et al., 2005 and Bes de Berc et al.,*  
108 *2005).*

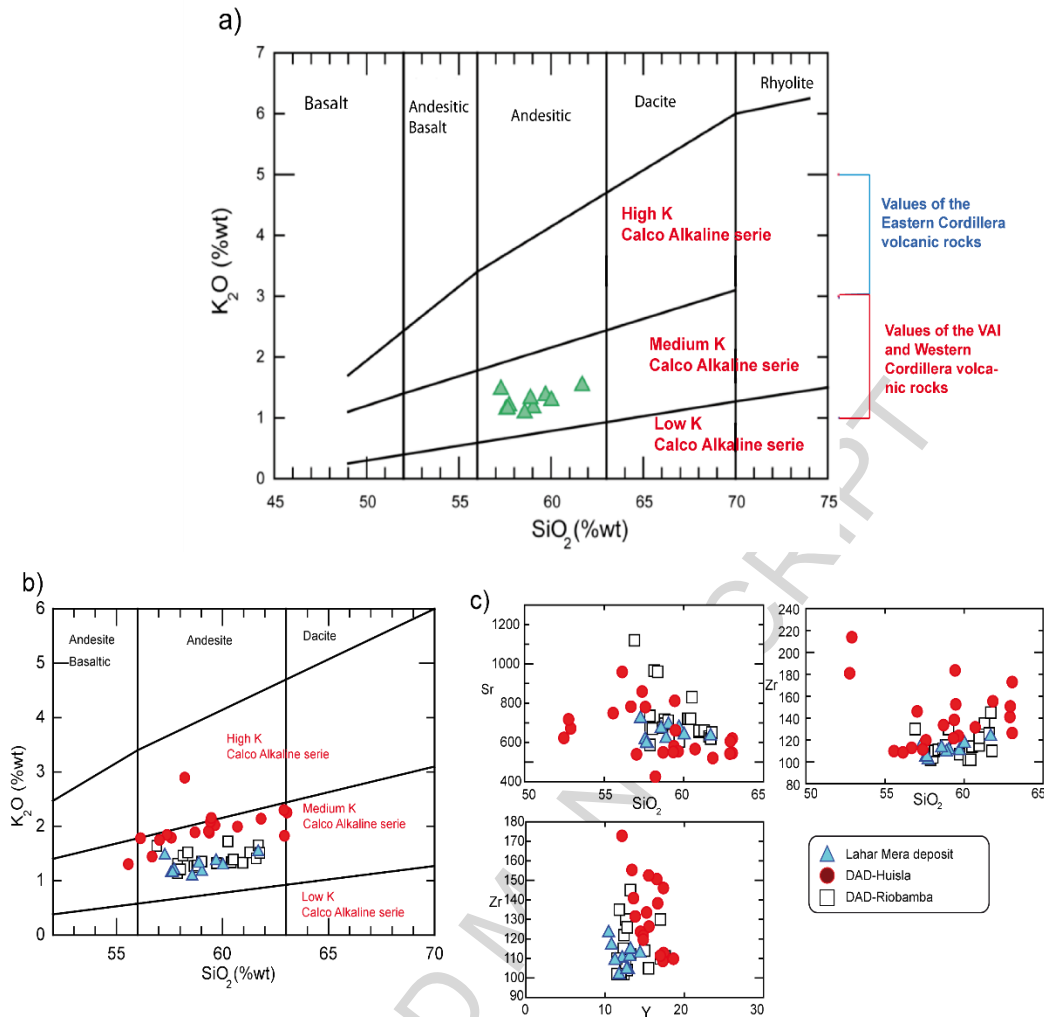
109  
110 **2.1.2 -Source of the Mera Lahar based on Geochemical and Petrographic Fingerprinting**  
111

112 In order to determine the source of clastic material of the Mera lahar we examined fresh and  
113 unweathered rocks from several volcanoes in the Pastaza discharge basin and compared them with  
114 the petrography of representative clasts extracted from Mera lahar deposit. The petrography of lithic  
115 clasts within Mera lahar is principally a light to dark gray, porphyritic to aphanitic andesitic rock. The  
116 general mineral assemblage is plagioclase, pyroxene (clinopyroxene and orthopyroxene) with scarce  
117 hornblende in a gray pinkish microcrystalline matrix.

118  
119 Whole-rock analysis shows that Mera lahar is principally comprised of andesites ranging from 57 to  
120 61 wt% SiO<sub>2</sub> that plot in the medium K calc-alkaline series (containing 1 to 1.5 wt% K<sub>2</sub>O). Rocks from  
121 volcanoes located on the Eastern Cordillera (EC) generally show higher K values than those located  
122 on the Western Cordillera (WC) (Schiano et al., 2010). (Figure 4a), a pattern due to the overall greater  
123 differentiation of magmas in the EC (Barragán et al., 1998) (Fig. 4a). Rock compositions from the Mera  
124 lahar suggest that the source could be in the WC, due to its lower K values. Following this line of

125 evidence the potential volcano sources of the WC for the Mera lahar debris flow would be  
126 Chimborazo and/or Carihuairazo volcanoes (Fig. 2). While from the EC the volcano candidates would  
127 be: Huisla, Tungurahua and Altar volcanoes and Quiñuales massif (see Fig. 2). Nonetheless, except  
128 for Huisla and Chimborazo rocks, characteristics of samples from other possible source volcanoes steered  
129 Espín (2014) to reject them as source candidates because of: lower potassium values for Carihuairazo  
130 rocks; overwhelming presence of hornblende in Altar rocks; the young, recent age of Tungurahua  
131 DAD events, and the more basaltic composition of Quiñuales rocks.

132  
133 In Figure 4a we observe in samples from Mera Lahar that  $K_2O$  presents a positive correlation when  
134 plotted against silica ( $SiO_2$ ) whereas trace element, Sr, Ni, Cr, V, Co, Y, Yb, Gd, Dy, Eu, and Nb have a  
135 negative correlation with increasing silica content. On the contrary, Ba, Rb, Zr, Th, Nd, La y Ge present  
136 a positive correlation (Supplementary Data\_1). Overall these elements form a non-dispersed field  
137 which implies that they are likely of only one source.



138  
139

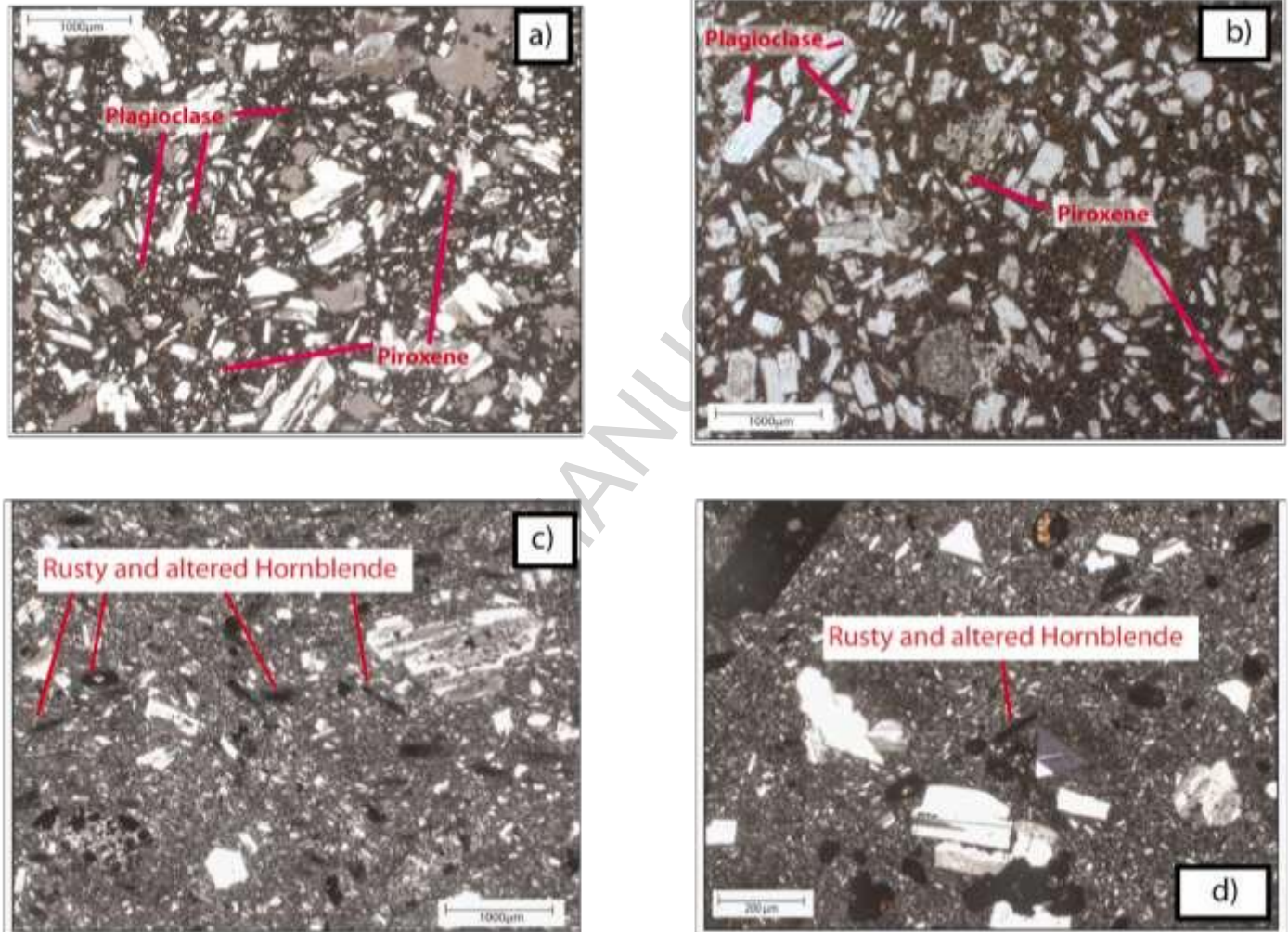
140 *Figure 4. Volcanic rock classification diagrams and insertion of the Mera lahar rocks. a)  $K_2O$  wt% vs.  $SiO_2$  wt% (Peccerrillo*  
 141 *and Taylor 1976). A clear distinction is made between rocks of the Eastern and Western cordillera (Schiano et al., 2010).*  
 142 *b) Trace elements variation diagrams, major elements vs.  $SiO_2$  wt%. c) Comparison between the Riobamba and Huisla*  
 143 *avalanche deposits as potential source candidates for the Mera lahar deposit.*

144

145 Our geochemical study exhibits a correlation between rocks of both the Mera lahar and rocks from  
 146 debris avalanche deposits, of Huisla and Riobamba (Chimborazo volcano), Samaniego et al., 2012,).  
 147 A correlative relationship is represented in the Harker diagram (Fig. 4b). With respect to major  
 148 elements, differing trends cannot be distinguished between the possible source volcanoes since the  
 149 samples fall closely together in plots exhibiting  $SiO_2$  vs trace elements (Sr, Zr or Y) (Fig. 4c) and the  
 150 tendencies are almost indistinguishable. Geochemistry of Tungurahua DAD rocks is not discussed  
 151 here as these events are younger than the Mera lahar, which has a  $^{14}C$  date greater than 40 ka (see  
 152 section 4.1.2).

153

154 Alternatively, petrographic comparison between clasts from Mera lahar with clast samples from the  
 155 possible source volcanoes suggests the source option as Huisla volcano DAD rocks. Rocks from both  
 156 Mera lahar and Huisla avalanche deposit share a similar mineral paragenesis (plagioclase,  
 157 orthopyroxene and clinopyroxene). The similarities are also seen within the phenocrysts and the  
 158 matrix (Fig. 5a).



159  
 160 *Figure 5. a) Thin section made from andesite clast from Huisla-DAD shown with crossed nickles, showing the plagioclase,*  
 161 *pyroxene and opaque minerals. b) Thin section from representative clasts from Mera Lahar deposit showing mineral*  
 162 *association: plagioclase > clinopyroxene >> orthopyroxene >> opaque minerals. c) Thin section of rock from Riobamba DAD*  
 163 *with nickles crossed from Samaniego et al., (2012), differs from the Mera lahar rocks by having fewer plagioclase crystals*  
 164 *and the presence of oxidized and altered hornblende. d) View of thin section with crossed nickles (Riobamba DAD) of*  
 165 *oxidized hornblende, plagioclase crystals and the matrix.*

166

167

168 As stated above, geochemically Chimborazo volcano rocks of the Riobamba DAD (Samaniego et al.,  
 169 2012) are also akin to rocks in Mera lahar. However, the higher percentage of plagioclase crystals and  
 170 the presence of oxidized and altered hornblende crystals in Chimborazo rocks (Fig. 5cd) differ  
 171 significantly from those in all samples of the Mera lahar rocks (Fig. 5ab), as observed by Espin (2014).

172 To further strengthen our choice of source rock for the Mera lahar, additional spot sampling was  
 173 undertaken at ten Riobamba DAD outcrops. Altered hornblende crystals were apparent in clasts  
 174 removed from the avalanche deposit, as opposed to the fresh, but scarce hornblende crystals present  
 175 in Mera lahar lithic clasts.

176

### 177 3.1 Results

178

#### 179 3.1.1 Huisla Volcano, Source of Mera Lahar

180

181 Huisla volcano is located 6.5 km south-southwest of Pelileo and 13 km to the south- southeast  
 182 of

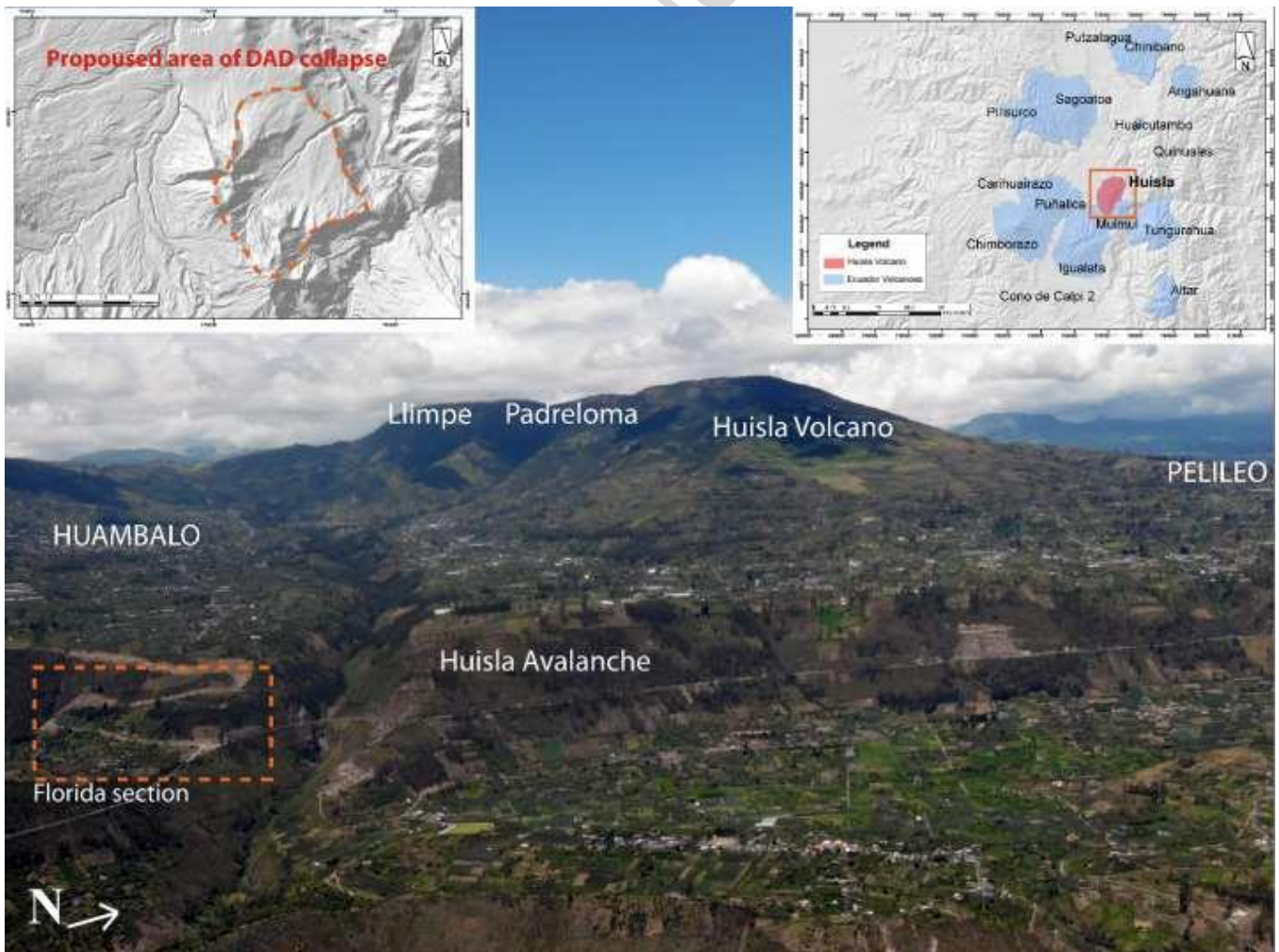
183

184 Ambato and is part of a low-lying volcanic complex which consists of three main peaks: Huisla (3763

185

186 m.), Llimpe (3732 m.) and Padreloma (3650 m) (Fig. 1, 2 & 6).

187



188

189 *Figure 6a. Huisla volcano's edifice and surrounding area, with main towns Pelileo and Huambalo. View is toward the west*  
 190 *and in the foreground is the nonbuttressed E and NE portion of the volcano, whose predecessor peak/dome had a sector*  
 191 *collapse, the breccias coming to rest in the valley bottom of the Patate River at base of photo. La Florida section is*  
 192 *highlighted. The low pass left of Llimpe peak is cut by a regional transpressive SW-NE striking fault. Inset on left concerns*

193  
194

*the area of proposed collapse of Huisla. Inset on right shows Huisla in relation to other nearby volcanoes in the upper Pastaza drainage basin. Huisla's coordinates are: UTM- 0770930/9847616.*

ACCEPTED MANUSCRIPT





196

197 *Fig. 6b. View S-SW of Huisla's central peak, which regrew inside the remaining concentric walls after collapse. Multiple*  
 198 *meter thick post-collapse rhyolitic ashfall layers outcrop below the highway on the opposite side of the valley from Totoras*  
 199 *town. Pachanlica stream runs at the base of the rhyolitic tephra fall units.*

200

201 The Huisla volcanic complex is built upon rocks of the Cisan volcanic formation of Miocene age  
 202 (Bustillos, 2008) and is mainly composed of calco-alkaline andesitic rocks of medium potassium (K)  
 203 and basaltic andesites of low potassium. Petrographically they are porphyritic andesites whose  
 204 mineral association consists of plagioclase >> clinopyroxene > orthopyroxene, scarce hornblende and  
 205 presence of Fe/Ti oxides that are usually distributed in a microcrystalline matrix with interstitial glass.  
 206 Few studies have been made of Huisla and due to its subdued topography, the volcano commands  
 207 little attention.

208

209

210

212 Our studies on Huisla were conducted with the objective to identify the source of Mera lahar.  
213 Following the sector collapse the volcano erupted rhyolitic magmas resulting in the deposition of  
214 several white pumiceous high silica (73-75 wt% SiO<sub>2</sub>) tephra falls and pyroclastic flow layers on the  
215 western, northwestern and northern flanks which overly the avalanche breccia layers (Fig. 6 & 7).  
216 Evidence for bimodal eruptive activity (varying between andesitic to rhyolitic) is not observed in  
217 deposits comprising the pre-collapse Huisla flanks, therefore we hypothesize that the sector collapse  
218 decapped the magmatic system and could have facilitated the eruption of the high silica magma.  
219 Huisla's new edifice regrew and now occupies the base of Huisla's caldera-like structure (Fig 6b). A  
220 late Pleistocene age is assigned to the collapse based on younger ages of two overlying fine-grained  
221 rhyolitic tephra falls sourced to a vent in the Pisayambo area to the northeast (Mothes and Hall, 2008)  
222 and which are dated with the <sup>14</sup>C method as between 20 – 40 ka (Fig. 7).

223

224 Huisla's presumed low elevation summit would not have supported growth of permanent Pleistocene  
225 glaciers of Late Glacier Maximum (LGM) age and no moraines are found on Huisla's older flanks.  
226 Neighboring Iqualata volcano (4430 m asl), 15 km to the southwest, however has well-defined Late  
227 Glacier Maximum moraines (Hastenrath, 1981) that extend to below 4000 m asl elevation. More  
228 likely is that periglacial conditions likely existed on Huisla's former summit, fostering local bogs and  
229 some ground ice. Without significant summit glaciers during the Late Glacier Maximum, little if any  
230 in-situ superficial water would have been available to contribute to subsequent lahar formation,  
231 unless a small crater lake had been present.

232

233

234

235

### 3.1.2 -Huisla Stratigraphy

236

237

238

239

240

241

242

243

There are two prominent debris avalanche breccia layers exposed in the La Florida outcrop (Fig. 6a & 7). Layer AV1 is without ballistic bombs, while AV2 displays abundant radially fractured bombs. A lithic fall layer lies between them (Fig. 7). Adjacent to La Florida outcrop a Cangahua layer caps the lithic-rich layers and is overlain by several white pumice lapilli fall layers whose thickness exceeds 1 meter. Cangahua is a regional indurated fine ash accumulation of Pleistocene-age (Clapperton, 1990). In some places the top part of the stratigraphic sequence is also covered by a prominent lithic–scoria fall deposit from Tungurahua volcano (Fig. 7). Dating by the  $^{14}\text{C}$  method of small charcoal pieces in the ashy medium associated with the top scoria layer provided a date of ca.9 ka (Bustillos, 2008; Le Pennec et al., 2013).

244

245

246

247

248

249

250

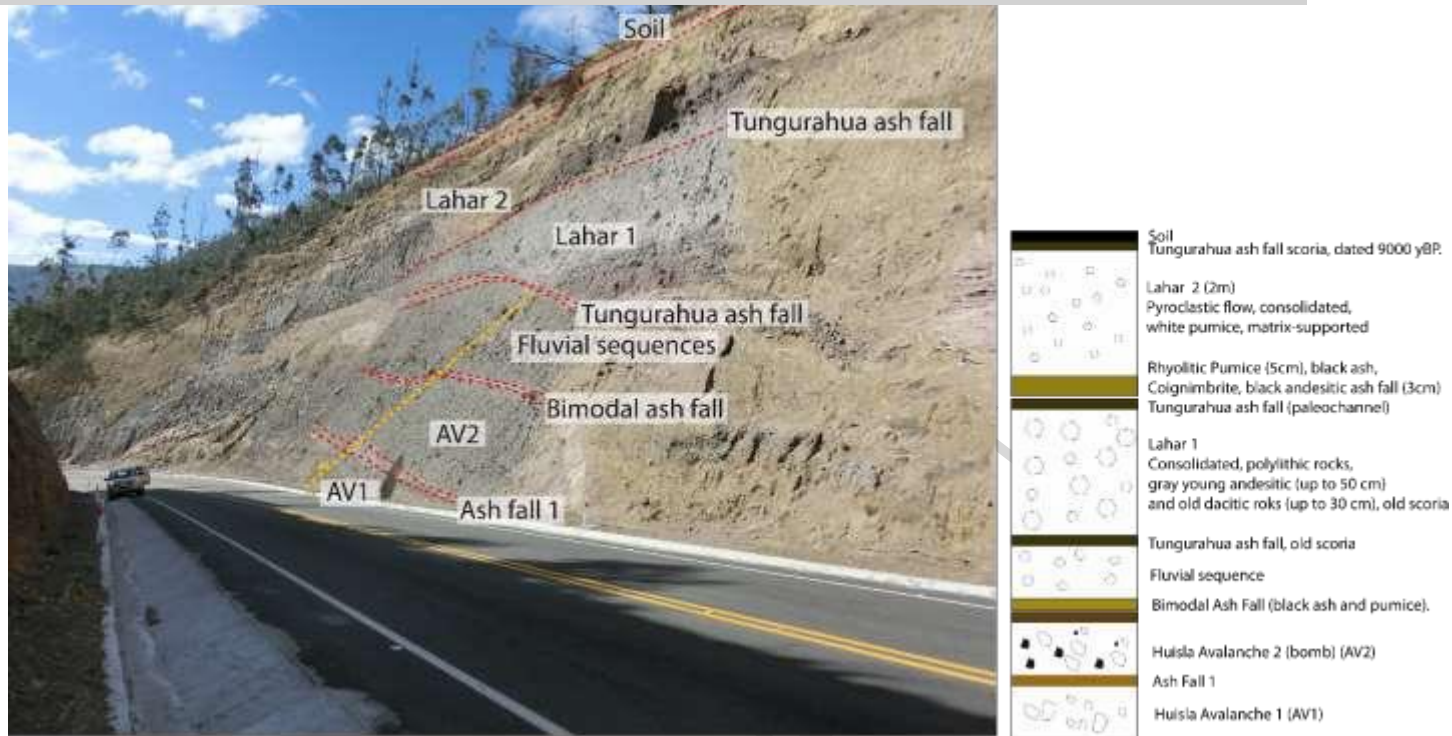
251

252

253

254

On the northwest flank of the volcano (above Totoras town, Fig. 6b), thick pyroclastic flow deposits outcrop between the principal tephra fall layers that are of rhyolitic composition (Fig. 6b). Huisla volcano is cut on its SW flank by the trace of a regional transpressive strike-slip fault, known as the Chingual-Cosanga-Pallatanga-Puná (CCPP) fault (Alvarado et al., 2016). The CCPP fault enters the study area from the southwest creating morphological displacements of young strata on neighboring Iguata volcano. The fault's trace through Huisla's SW flank roughly aligns with the southern boundary of the sector collapse scar (Fig. 6ab). The same fault trace crosses the Patate River canyon, trending northeast into the Llanganati-Pisayambo area. Sheared topography and meter range displacements on Younger Dryas glacial stage moraines are observed, as are small, but frequent ground displacements detected by InSAR eastward of Pisayambo lake (Champenois et al., 2017).



255

256 *Figure 7. Geological sequence at La Florida area (see Fig. 6a for location) where it is possible to see two layers of Huisla*  
 257 *debris avalanche deposit (AV1 & AV2), several ash fall layers and lahar deposits. The rhyolitic tephra falls so prominent at*  
 258 *the Totoras section (Fig. 6b) are poorly preserved at this outcrop, which is cut by a regional transpressive fault, observed*  
 259 *in Fig 6b. The cross-cutting yellow line represents the fault trace.*

260

### 261 **3.1.3 -The Huisla Debris Avalanche Footprint**

262 The Huisla DAD underlies Pelileo, Patate, and Pingue towns and notably outcrops along the Pelileo-  
 263 Baños highway (Fig. 6b). It can also be found outcropping on the E side the Patate River in the barrio  
 264 of Tauwicha, situated some 830 m above the Patate valley bottom. Our field mapping shows that the  
 265 DAD covered an area of approximately 150 km<sup>2</sup> with an average thickness of about 50 m and whose  
 266 volume is estimated in 4 km<sup>3</sup> (Espín, 2014; Espín et al., 2015). (Figure 2). Huisla's older eroded flanks  
 267 that comprise the south, northwest and western rims once encircled a former peak/dome of Huisla  
 268 and which, based on projection of the present morphology, had a volume of approximately 4-5  
 269 km<sup>3</sup> before flank failure (Fig. 6b).

270

271 Provoked by Huisla's flank failure the avalanche breccias from the peak/dome slid down the  
 272 unbuttressed east and northeast flanks and lodged in the canyon bottom of the Cutuchi–Patate River  
 273 south to the union with the Chambo River, at Tungurahua volcano's base (Fig. 1 & 2). The Panchanlica  
 274 River channel north of Huisla and now occupied by the northern portions of Pelileo, Totoras, and  
 275 Salasaca towns may also have received Huisla DADs, but evidence is meagre (Fig. 1 & 6b)

276

## 277 **4.1 Deposits of Mera Lahar**

### 278 **4.1.1 -Deposit Description**

279

280

281

282

283

284

285

286

287

288

289

290

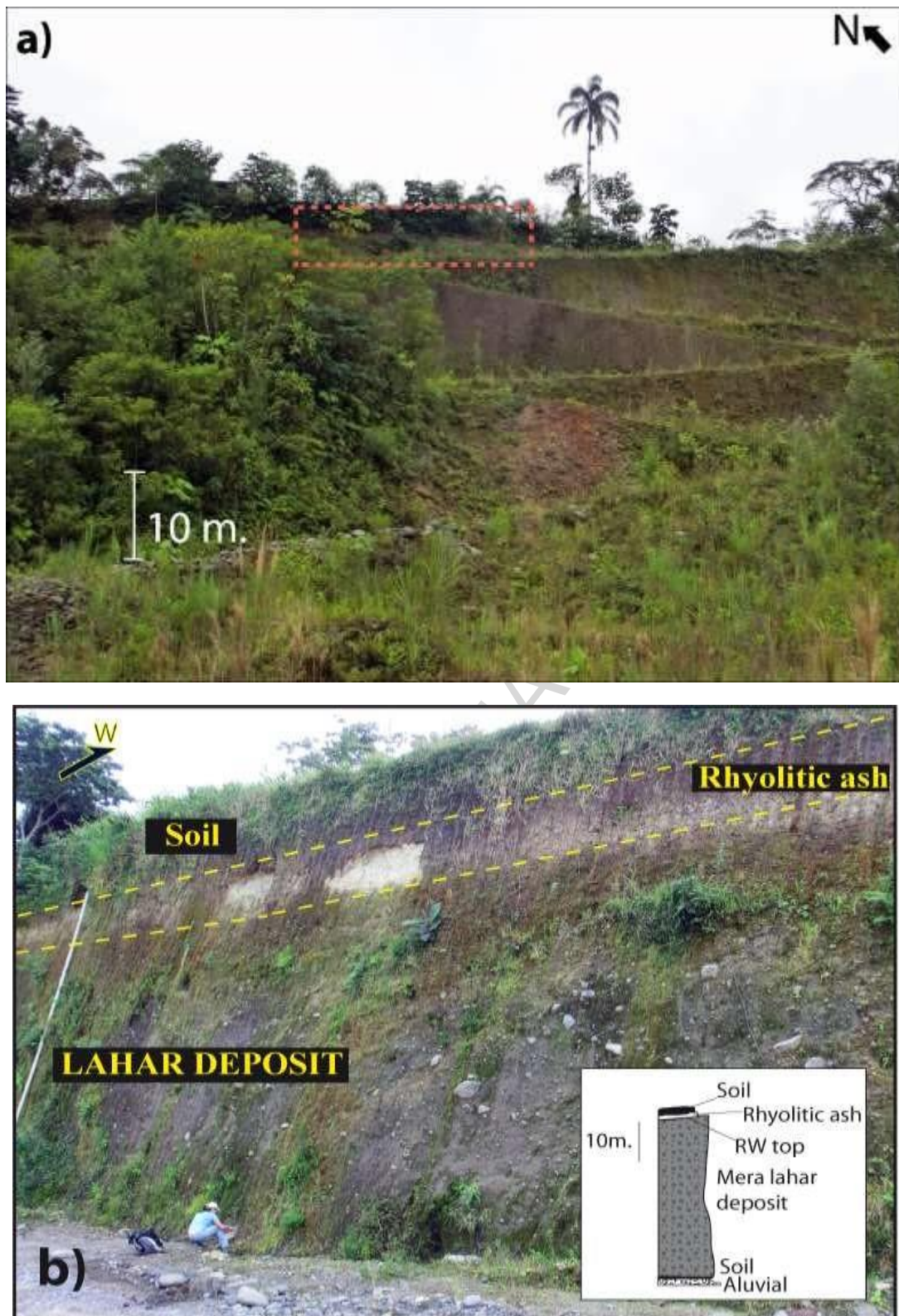
291

292

293

In the main depositional zone along the Pastaza River, east of El Topo town (Fig. 1 & 3), the Mera lahar deposit underlies a 2 m thick layer of tropical brown soil or alternatively, river cobbles in most outcrops. In Moravia, Pindo and Madre Tierra towns a layer of rhyolitic ash fallout with a thickness of 60-70 cm (Figure 8ab) overlies the reworked top of the lahar deposit. The base of this ash layer is dated at ca. 20 ka at a cut near Mera dike (a natural swimming pool, 1 km E of Mera town, see Fig. 3) (Keen, 2015), and its provenance is believed to be the Pisayambo area 40 km northwest, where large siliceous eruptions occurred in the late Pleistocene (Mothes and Hall, 2008). Bulk major and trace element geochemistry shows good correspondence between this marker rhyolitic ash layer and the suggested Pisayambo source (Table 1 and Supplemental data\_2). In contrast, at an important cut 0.5 km downstream from Mera dike the lahar is overlain by a 12 m thick accumulation of intercalated organic layers, mainly peat, tephras and also granitic stream cobbles.

Deposition on top of the flat poorly-drained Mera lahar favored long-term swampy conditions and isolation from flooding, as described by Keen (2015).



295  
 296 *Figure 8. a) Outcrop of Mera lahar deposit in an abandoned quarry located 15 vertical meters below the fire brigade station at*  
 297 *Moravia. Box at top of photo indicates location of photo 8b. b) Lithological section at the same quarry showing a few 20-30 cm*  
 298 *diameter clasts in a gray-fawn-colored matrix. A rhyolitic ash layer is located near the top of the reworked top of the lahar deposit.*  
 299 *Inset is an abbreviated stratigraphic column in which the Pastaza alluvium underlies the lahar deposit.*  
 300

303

304

305

306

#### 4.1.2 –Dating of Mera lahar and Overlying Strata

307

308

309

310

311

312

313

314

315

316

An earlier study by paleontologists Lui and Coolinvaux (1985) reported a major lahar deposit 2 km west of Mera town where two organic layers on top of the lahar gave radiocarbon ages of ca. 26 ka and 33 ka. Later, Heine (1994) reported radiocarbon ages of 33.7 and 40.6 ka for two overlying peat layers found in a cut between Mera and Pindo Mirador towns. Finally, Bès de Berc et al., (2004) presented two ages of ca. 41 ka and ca. 18 ka for organic layers overlying the lahar along the Mera-Baños highway cut. For this study, and based on Espin, (2014), we report a new radio carbon age of >43.5 ka for a tree trunk pulled out of the Mera lahar deposit (Table 1). Table 1 is a compendium of all known age dates for deposits overlying the Mera lahar. All of the age dates (uncalibrated) ranging between about 17 ka to 40.5 ka relateto organic strata overlying the Mera lahar and therefore provide a minimum age for the stratigraphically lower (underlying) Mera lahar (Table 1 & Fig. 9).

Site & UTM Coordinates	Unit dated	Date Collected	Material dated	Conventional age (BP); Laboratory	Calibrated Age- cal yr BP, 2 sigma	Reference
Mera Dike East Organic layer "O"  underlies fine-grain rhyolitic ash (Sample MERA2YTEPH1 with pumice lapilli layer on top. (72.93 wt% SiO <sub>2</sub> & 4.2 wt% K <sub>2</sub> O). 500m downstream of Mera Dike. UTM (17M) 822352/983857 1118m	Organic layer "O" at ~100 cm depth & ~11 mts above Mera lahar top.	04 Sept. 2012	Pollen residual in Macro-Fossils.	16,690 ±60 AMS  Beta Analytic ID # 397417	19,965-20,215	Keen, 2015
Mera Dike East	Organic layer "N" at 185 cm depth; overlies tephra MERA2YTEPH2	04 Sept. 2012	Wood	28,580 ± 140	31,877-33,058	Keen, 2015
Mera Dike East Organic Layer "I"  at 665 cm depth, and ontop Mera Lahar, 6 m lower. 500 m downriver of Mera Dike. UTM 822352/983857 1118m	Organic layer "I" at 665 cm depth; provides maximum date for Tephra layer, MERA2YTEPH3 (67.53 wt% SiO <sub>2</sub> & 2.64 wt% K <sub>2</sub> O).	04 Sept. 2012	Pollen residual in macro fossils.	39,500 ± 270 AMS  Beta Analytic ID # 411030	42,702-43,683	Keen, 2015
Mera 1 site, near Rio Pastaza/Rio	Vegetal (peat) layer overlying	1991	Peat	33,670 ±520 Lab unknown	34,582-37.311	Heine, 1994

Alpayacu confluence. In highway cut on N side, after crossing Rio Alpayacu. UTM 822363/983750 1082m	Mera lahar.					
Mera 1 site, near Rio Pastaza/Rio Alpayacu confluence. In highway cut on N side, after crossing Rio Alpayacu. UTM 822363/983750 1082m	Tree trunks and branches on top of underlying Mera Lahar	1991	Wood	40,580±1220 Lab Unknown	40,472- 44,882	Heine, 1994
Mera-Baños highway. UTM 819848/983941 1114m	Peat layer, 10 m below top and overlying Mera lahar.	July 29, 2002	Organic layer/ Peat	40,580±1030 Radiometric Beta Analytic ID # 169315; Sample MERA 240702	40,692- 44,238	Bes de Berc et al., 2004
Moravia fire brigade station quarry, UTM 824919/9835442, 1902masl	Mera Lahar interior.	30 July 2011	Tree trunk from lahar's interior	>43,500 Radiometric Beta Analytic ID # 366381		Espín, 2014

317

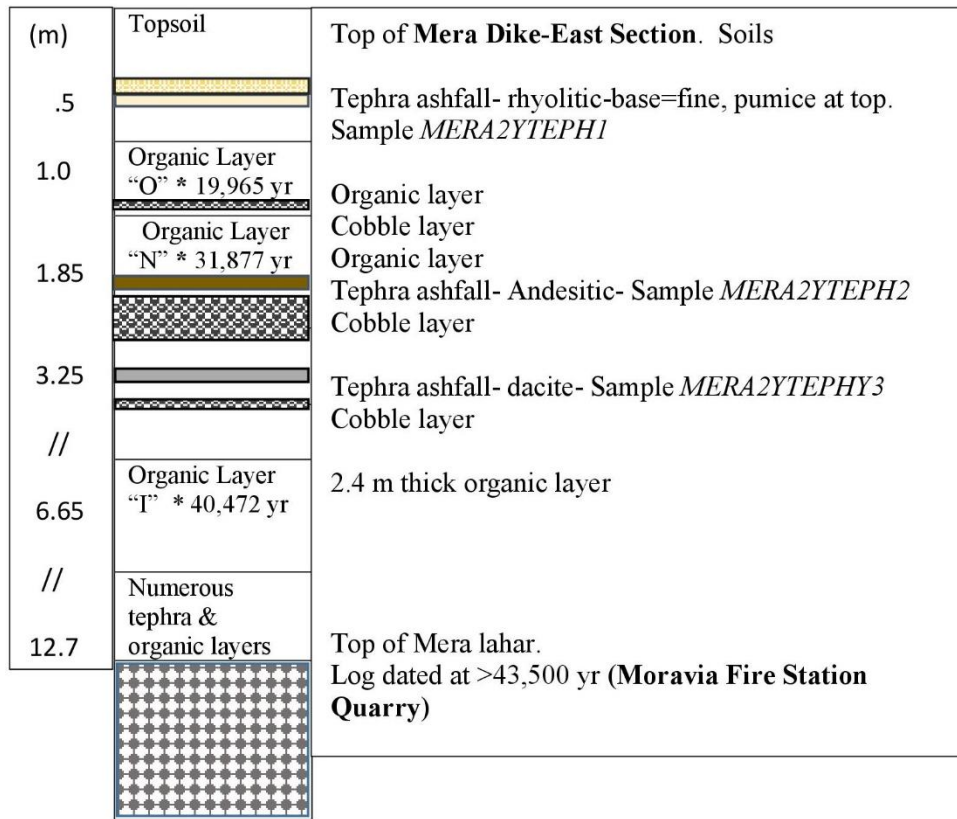
318

319

Table 1: Radiocarbon dates for organic layers overlying the Mera lahar and also from the lahar's interior.

320





321

322 *Figure 9: Simplified stratigraphic column for the Mera Dike East section UTM 822352/983857, 1118 m asl and located 0.5*  
 323 *km downstream of Mera dike swimming area. <sup>14</sup>C dates from Keen (2015). Geochemical analysis of the three main tephra*  
 324 *layers that overly Mera lahar at Mera dike are presented in Supplemental Data\_2. Top tephra, MERA2YTEPH1 is a rhyolitic*  
 325 *marker layer of Pisayambo provenance (Mothes and Hall, 2008).*

326

327

### 328 **4.1.3 – Mera Lahar Componentry**

329

330 The Mera lahar deposit is primarily monolithologic and is best described as a matrix-supported breccia  
 331 (70%) of reddish gray color with angular and sub angular, gray and reddish andesitic clasts (Figure  
 332 10a-e). However, exogenous clasts, mainly granitic, outcrop at the base. Overall, sorting is poor--  
 333 millimetric grain size to clasts of >30 cm), although sand-size grains can be abundant.

334 The deposit's matrix is hardened and well-consolidated, but also displays molds and pores within the  
 335 matrix. The lahar's top surface tends to be indurated. In the middle of the deposit there is greater  
 336 alteration (oxidation) in the matrix. At the base there are more angular than rounded clasts (size:  
 337 decimeter to 1.5 m). Radially fractured bombs are occasionally found within the lahar's body and the  
 338 lahar also carried along cobble substrate as it bulked up while flowing downstream.

339

340

341



342



343 *Fig. 10. Composition of Mera lahar deposit. a) Meter-size clasts in the Moravia area, b) Characteristic andesitic clast of the*  
 344 *deposit. c) Reddish gray to fawn colored matrix is well-consolidated at Moravia quarry. d) Matrix in Motolo area. e)*  
 345 *Oxidized matrix at the Cumanda cut.*

346

347 At the deposit's base at Madre Tierra the clasts are surrounded by a matrix with poor sorting,  
 348 oxidation zones and granitic clasts that the lahar dragged along. Also the contact between fluvial lens  
 349 of the Pastaza river fan and the lahar deposit is sheared by reverse thrust faulting (Figure 11a). The  
 350 faults belong to a family of N-NE striking regional structures that absorb tectonic compression on the  
 351 E flank of the Cordillera Real (Pratt et al., 2005) (Fig. 3).



352 *Figure 11. Outcrop seen on the road to Madre Tierra. a) Presence of shear structures in the deposit due to local thrust faulting.*  
 353 *b) Oxidation zone in the matrix. c) Reddish gray matrix, andesitic clast and granitic clast in the lahar. d) Rounded clasts at the*  
 354 *bottom of deposit and the contact with alluvial cobbles of the Pastaza River.*

356 At Cumanda town, on the right margin of the Pastaza River, along the new road to Palora town, the  
357 deposit is embedded in a sequence that includes river deposits and abundant weathering and  
358 alteration is observed (Fig. 11b & c). Numerous metamorphic rocks (schists) belonging to the Eastern  
359 Cordillera basement complex are present, having been entrained along the flow route. At the  
360 deposit's base there are alluvial deposits with rounded Abitagua granitic clasts (Fig. 11d). Finally, a  
361 layer of rhyolitic ash, with similar mineralogy and texture to that observed at nearby Moravia, Mera  
362 and Pindo cuts (Fig. 8b; Fig. 9 & Table 1- see notes on MERA2YTEPH1 ash)), overlies the upper and  
363 reworked portion of the Mera lahar deposit at Cumanda.

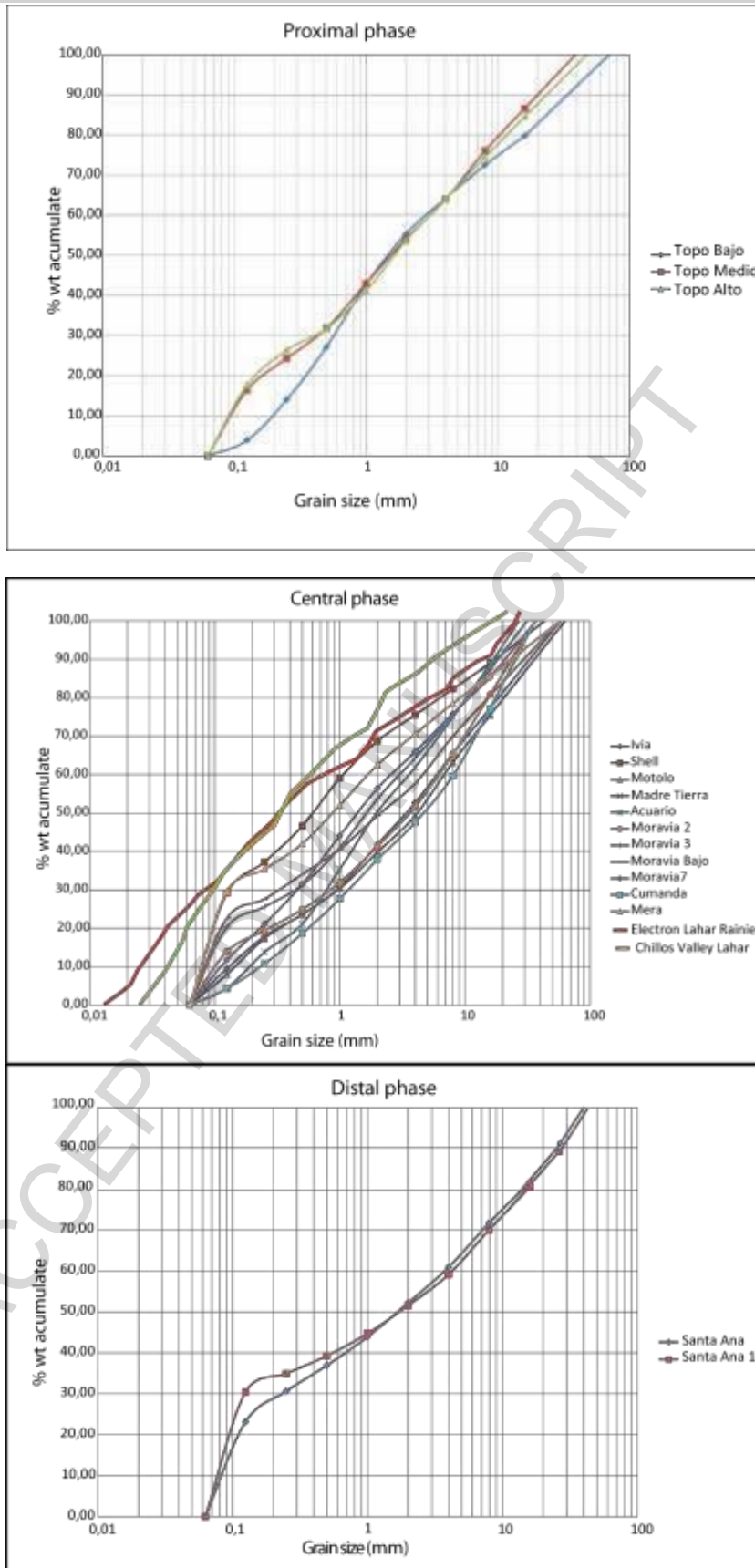
364

#### 365 **4.1.4 -Granulometry**

366 We provide granulometric parameters for 16 samples taken from the proximal, central and distal  
367 phases of Mera lahar deposit. Overall granulometry of the Mera lahar shows a distribution between  
368 fine grain particles of 0.06 to 1.0 mm with accumulations of 55% in the proximal phase samples, while  
369 in the central and distal phases grain sizes of 0.06 to 1.0 mm constitute between 28-60% and 45%,  
370 respectively of the samples. There is essentially no material finer than 0.06 mm, ie., an absence of silt  
371 and clay-size grains. The matrix comprised of grain sizes smaller or equal to 2.0 mm (coarse sand size  
372 granules) overall constitutes 60%, 40-70% and 50%, respectively of the three categories (Fig. 12).  
373 Grain sizes in the >2.0 – 100 mm range (gravel size) occupies about 40-50 % of the deposit for the  
374 three phases.  
375

376

377 Comparing the Mera lahar's granulometric values with those of Cotopaxi's Chillos Valley Lahar, a  
378 matrix-rich deposit that contains between 10-20% clay and silt-size grains in bulk deposits (Mothes et  
379 al., 1998), and of the Electron lahar from Rainier volcano, USA, which has around 30% silt and clay-  
380 size components (Scott and Vallance, 1995), we see that Mera lahar deposit overall has a higher  
381 percentage of coarser components in the sand and gravel categories.  
382  
383  
384  
385

386  
387

388

389  
390

391 *Figure 12. Granulometry of the Mera lahar matrix using data from 16 samples taken in proximal, central and distal zones.*  
 392 *Data for Electron lahar from Scott and Vallance (1995) and Chillos Valley lahar from Mothes et al., (1998).*  
 393 *Consult Fig. 1 & 3 for place name locations.*

394

395

396

### 5.1 Modeling the Mera Lahar

397

398

399

400

401

402

403

404

405

Employing the program LaharFlow (Woodhouse et al., 2016a) we simulated the flow path and inundation zones of the Mera Lahar. Laharflow is a computer code that uses equations from fluid mechanics for simulating lahars (see <https://laharflow.bris.ac.uk/?loginfailed>). Recently developed by the Earth Sciences and Mathematics departments of The University of Bristol (Woodhouse et al., 2016a), its input parameters include a digital terrain model (30 m actual DEM), flow rheology parameters such as Chézy roughness coefficients (turbulent fluid), Coulomb coefficient (flow granular e.g. Pouliquen, 1999) and Voellmy coefficient (fluid grains). These parameters were calibrated using the Nevado del Ruiz lahar's estimated volumes and flow hydrographs (Supplementary Data\_3).

406

407

408

409

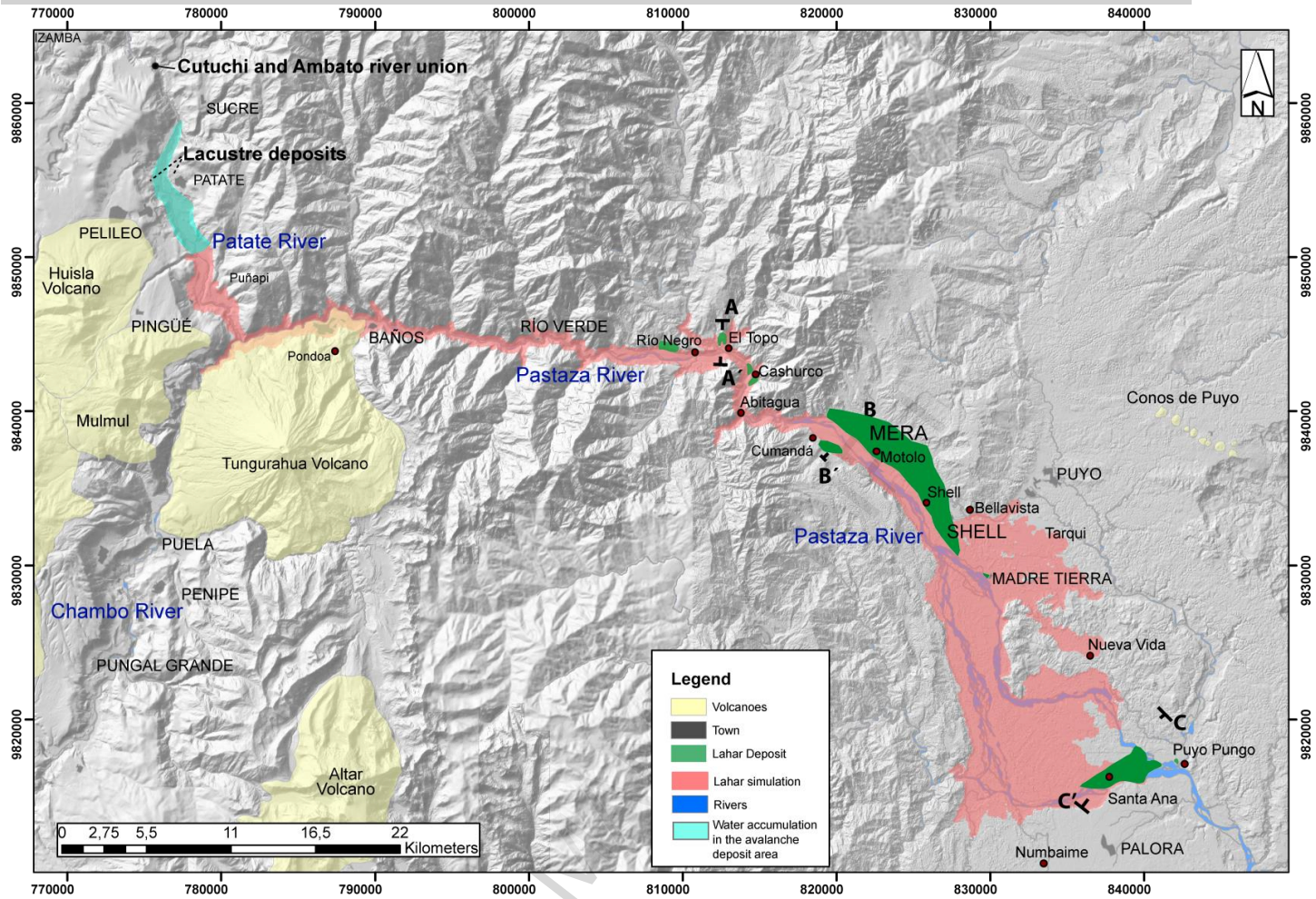
410

411

412

413

Simulation with LaharFlow takes into account mass and momentum conservation and kinetic energy. This program has now been used to simulate Cotopaxi's 1877 primary lahars and Tungurahua's secondary lahars of 2016 (Woodhouse et al., 2016b), and finally, the potential primary lahars that could flow down the east flank of Cayambe volcano, Ecuador (Espín et al., 2017). For modeling the Mera lahar, a total volume of  $5.4 \text{ km}^3$  was used (original avalanche breccia volume of  $4 \text{ km}^3 + c 1/3$  water). The transit begins with the breakage of a proposed temporary dam near to Patate, unleashing most of the water necessary to remobilize the avalanche breccia and bring about transformation to a voluminous lahar (Fig. 13).



414  
415

416 *Figure 13. Results of Mera lahar simulation using the LaharFlow program; total volume used was 5.4 km<sup>3</sup> (4 km<sup>3</sup> of DAD*  
 417 *breccia and 1.4 km<sup>3</sup> of water). (Google Earth Base). The turquoise-colored area near Patate represents the zone of ponded*  
 418 *water accumulation in the avalanche deposit, while the pink color is the lahar's modeled inundation footprint. The dark*  
 419 *green shapes are approximate limits of remnants of the mapped Mera lahar deposit. Sections AA', BB' and CC' refer to*  
 420 *topographic profiles discussed in figure 15.*

421

422 We hypothesize that the failure of the temporary dam in the DAD breccia could have occurred due to  
 423 shaking by a local earthquake, pore pressure threshold failure in the dam wall, overtopping, etc, and  
 424 that the ensuing rupture resulted in a watery avalanche breccia that incorporated available water and  
 425 was transformed to a potent secondary lahar. Due to the steep gradients (5%) in the Pastaza river  
 426 canyon between Baños and Rio Negro town, perhaps the Mera lahar was not deposited in this stretch,  
 427 since no deposits are observed.

428 The lahar traveled down the Pastaza River and began major deposition where the Pastaza canyon  
429 widens at Rio Negro town, then it again experienced choked flow in the Rio Topo area, south of Rio  
430 Negro. Here westward verging reverse thrust faults cut through granites in the El Topo area (Bes de  
431 Berc, 2005; Pratt et al., 2005; Bernal et al., 2012; Alvarado et al., 2016), effectively lowering gradient  
432 in the Pastaza river channel. Terraces 30-50 m high comprise the first mapped Mera lahar deposits  
433 found between Rio Negro and El Topo towns (Fig. 13).

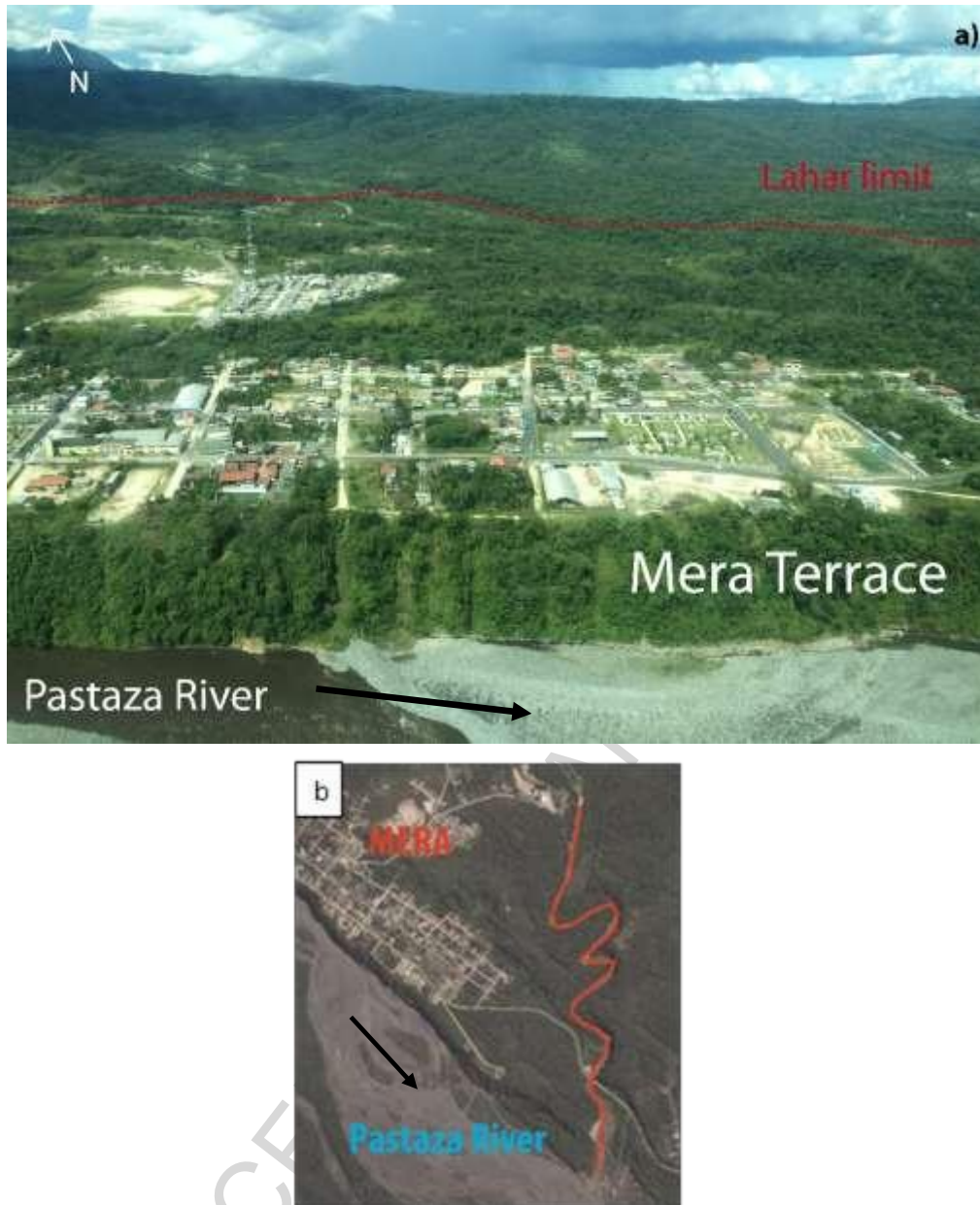
434

435 Once passing the constriction of the Abitagua batholith, the flow burst out onto the lower gradient  
436 Sub- Andean zone and the lahar's footprint became increasingly wider to the east-southeast of Mera  
437 (Fig. 13) and deposited along the paleowalls of the Pastaza River channel as well as invading side  
438 valleys and braided channels associated with the lower Pastaza River (Fig. 13). Subsequent and  
439 ongoing erosion by the Pastaza River left prominent stranded terraces on either side of the Pastaza  
440 (Fig. 14a), i.e. the surfaces where the towns of Mera and Shell are situated. These high stand terraces,  
441 with their indurated lahar core now control the drainage patterns of incoming streams, such that  
442 secondary streams run parallel to the Pastaza River before finally cutting through the indurated Mera  
443 lahar surface to reach local base level of the Pastaza River. One such example is that of the Alpayacu  
444 River which makes 3 hard bends before joining the Pastaza River (Fig. 14b).

445

446 Southeast of Shell town the Pastaza channel widens to several kilometers and verves eastward. Bernal  
447 et al., (2012) provide evidence of changes in the main course of the Pastaza River along this 20 km  
448 stretch, particularly for migrations on the river's left margin when the main Pastaza pirated into the  
449 channel of the neighboring Puyo River in 1906 and 1976 near Tarqui town (Fig. 13). Earlier avulsions  
450 of the main Pastaza River would have caused erosion and or burial of the Mera lahar and perhaps for  
451 this reason we do not find the lahar deposits in the zone of Tarqui and Nueva Vida (Fig. 13). Precisely  
452 in this zone our modeling shows the lahar's route and inundation zone. Bernal et al (2012) emphasize  
453 the importance of back tilting of the Pastaza's channel's gradient in order for the bulk of the river to  
454 leave its normal course. The back tilting, they suggest, is from westward verging thrust faulting,  
455 evidence of which we have seen and example at nearby Madre Tierra (Fig 11a). Field confirmation of  
456 the presence of Mera lahar deposit in the eastern lobe between Shell and Nueva Vida towns has been  
457 unsuccessful (Fig. 13).





458

459

460

461

462

463

Figure 14. a) Aerial photo of the Mera terrace with Mera town in the center on the left margin of the Pastaza River. Approximate outline of Mera lahar limits is shown in broken red line. b) Google image of the curvy route taken by the Alpayacu river (represented by solid red color) as it cuts through the indurated Mera lahar deposit over a distance of 1.3 km from near Mera dike to the Pastaza River channel. Black arrows in both a and b photos represent flow direction of Pastaza River

464

465

466

### 5.1.1 -Mera Terrace Heights along the Pastaza Canyon

467

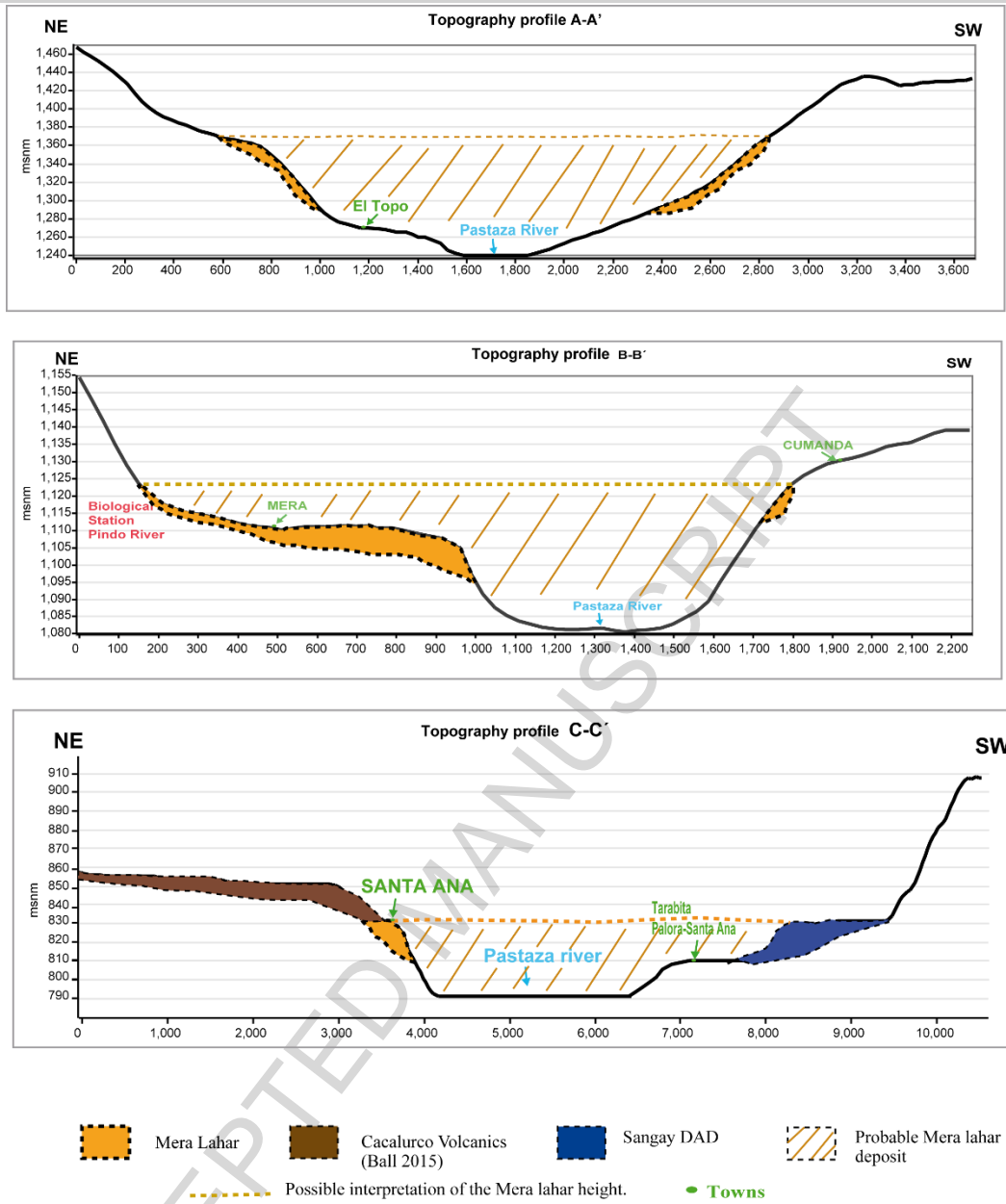
468

The lahar's high-standing terraces are particularly well identified at Mera, Shell and Cumanda, nearest to the mouth of the Pastaza canyon where they are 30-50 m above the actual river level (Fig. 15).

469 Further downvalley, both the Madre Tierra and Santa Ana terraces, which well display the Mera lahar  
470 rock suite and matrix, are of decreased height, apparently having suffered erosion. In the stretch  
471 between Mera and Santa Ana the lahar deposit's base overlaps preexisting Pastaza river alluvial  
472 deposits seen particularly well in the Moravia, Alpayacu and Madre Tierra outcrops.

473

474 The cross section AA (Fig. 13 & 15A-A') between El Topo town and the opposite side of the Pastaza  
475 River channel measures 2.2 km wide and lahar depositional thickness is 70 m. Between Cumanda and  
476 Pindo Biological Station, section BB has dimensions of 4.5 km wide and lahar thickness is 30 m (Fig.  
477 13 & 15B-B'). At Santa Ana, the deposit's farthest studied site, the lahar had a width of 4.5 km (Fig.  
478 13 & 15C-C') and is where a stratigraphic relationship can be seen between Mera lahar and the  
479 Cacalurco volcanics on the left margin and the younger DAD of Sangay volcano on the right margin.  
480 To the southwest of Santa Ana the younger Sangay volcano DAD (Valverde et al., 2015) presumably  
481 buried the Mera lahar deposit, which is well represented on the opposite side of the Pastaza, but  
482 we do not see Mera lahar outcropping on the SW bank. The Sangay avalanche occurred  
483 approximately 29 ka, (Valverde et al., 2015), thus confirming the older age of the underlying Mera  
484 lahar (Fig. 15C-C). These cross sections ratify not only the astounding height but also the broad lateral  
485 extent of the lahar compared to the actual Pastaza river channel.



486  
487

488 *Figure 15. Topographic x-sections showing the interpretation of the current distribution of Mera lahar deposits. On the Y*  
 489 *axis are the elevations above sea level in meters, while the X axis represents horizontal distances in meters. All placements*  
 490 *of Mera lahar and relationship with other features are based on field mapping. Note variable scales for each cut.*

491

492 **6.1 DISCUSSION**

493

494

495

496

497

498

499

500

501

502

503

504

505

506

507

508

509

510

511

512

513

514

515

516

517

518

519

520

521

522

523

Breccias related to the sector collapse of Huisla, a non-descript, little studied volcano on the central Ecuadorian Andean landscape provided the bulk of the clasts and matrix for the Mera lahar. We base the correlation between Mera lahar and the Huisla DAD on strong petrographic similarity between the plagioclase, clinopyroxene - orthopyroxene crystal assemblage observed in the clasts of both the Mera lahar rocks and the Huisla breccias. While the whole rock geochemical signatures of these two rock families are similar they are also akin to the Chimborazo avalanche breccias. The Chimborazo DAD rocks however have a high concentration of altered hornblende crystals, which are not characteristic to rocks found in the Mera lahar or in Huisla DAD clasts. Therefore, mineral fingerprinting was key to identifying the most likely source volcano as Huisla. Relative clast and crystal freshness and petrographic similarity of lithic clasts in the Huisla DAD deposit and equally so in the Mera lahar provided the convincing inputs. Additionally, no Mera-like lahar deposits are found in the upper part of the Chambo river valley alongside or downstream of Chimborazo avalanche deposit breccias (Bernard et al., 2008), even though there are wide valley stretches and stream inlets favorable for deposition and preservation. Neither are Chimborazo DAD deposits identified in the lower rio Chambo valley or near the intersection of the incoming Patate valley (Fig. 1). However, Huisla DAD outcrops are found all along the upper Patate River drainage (Fig. 1 & 2).

The presence of radially fractured fresh dome rocks in the avalanche breccia and also in the Mera lahar deposits suggests Huisla volcano had an active central peak/dome which subsequently collapsed. The dome rocks are very similar in mineral assemblage and composition both in the Huisla DAD and the Mera lahar deposit. The collapse involved a volume of ca. 4 km<sup>3</sup> of the unsupported E-NE flank of Huisla's edifice which sharply abuts the 300 meter deep Patate River canyon. The triggering of the sector collapse could have been facilitated by shaking from a local shallow earthquake on the active fault that cuts under Huisla's SE shoulder or to violent volcanic activity. As shown in figure 7, a lithic fall is associated with a respite between the two avalanche deposits. A blast deposit has not been identified.

As evidence of the post avalanche damming and resultant lake conditions, two packages of lacustrine deposits, each some 15 m thick are observed at the union of the Ambato and Cutuchi-Patate River

524 and also just below Pelileo town, both deposits which we believe may be the result of the Huisla DAD  
525 blocking the river course (Fig. 2). Following accumulation of  $\geq 1 \text{ km}^3$  of water, the dam broke and  
526 provoked a great flood/slurry. Other incidences of accumulation of  $> 1 \text{ km}^3$  behind temporary  
527 impoundments blocked by DAD material was noted by Capra (2006) who showed that well-sorted  
528 fine material in a DAD of mixed facies that constitutes a dams' interior may experience internal  
529 erosion by piping, thus accelerating dam failure. The mixed facies and matrix-predominance of the  
530 Huisla DAD where it slid into the Patate River canyon and effectively blocked the channel could have  
531 been a factor in accentuating the destruction of the temporary dam by overflowing.

532

533 We hypothesize that the mixing of Huisla avalanche debris and the accumulated water effectively  
534 transformed into the Mera lahar. In order to remobilize between 3 or more cubic kilometers of solids,  
535 at least  $1 \text{ km}^3$  of water would have been necessary (Vallance and Iverson et al., 2015). Assuming an  
536 efficient dam, it would have taken about 600 days to accumulate a reservoir of  $1 \text{ km}^3$  water volume  
537 using present discharge rates for the Patate River of ca.  $50 \text{ m}^3/\text{sec}$ . Flow was restricted within the  
538 large Pastaza canyon and deposition didn't begin until arriving to the widened sector at Rio Negro- El  
539 Topo towns (Fig. 1 & 3).

540

541 The lahar is remarkable for its matrix-rich, although non-cohesive nature that experienced little  
542 transformation downstream over the mapped 90 km distance. It's high concentration of sand-size  
543 particles may have retarded transformation to a dilute hyperconcentrated flow, as was also the case  
544 reported by Scott et al (1995) with some lahars at Mount St Helens. The almost total absence of clay  
545 size grains in the lahar is likely testimony to the lack of active hydrothermal alteration of the source  
546 volcano, but which is so common at Rainier volcano, and hence lahars borne from the flanks of Rainier  
547 where alteration is strongest have high clay-size content and hence were cohesive in nature (Scott  
548 et al (1995); Reid et al., 2001).

549

550 At Mera lahar's base, rounded river cobbles are incorporated, but within the central core, few  
551 exogenous rocks are seen. Precise dating of the Mera lahar has been unsuccessful, since a tree trunk  
552 pulled from its interior gave a date older than 43.5 ka and overlying dated organic units also range in  
553 age from earlier to ca. 40 ka, while a marker rhyolitic ash layer that is found near the top of a  
554 stratigraphic section at Mera dike is dated at approximately 20 ka, and the overlying Sangay DAD is  
555 dated at ca. 29 ka (Table 1: Fig. 9; Fig. 15C-C).

556

557 One of the most remarkable aspects of the Mera lahar is the preservation of the high-standing  
558 terraces which are situated well above the Pastaza River. Given that more than 40 ka have passed  
559 since the lahar's passage, the overall field mapping and verification of the deposit in this heavily  
560 vegetated and erosive zone was complex. We successfully employed the program LaharFlow  
561 (Woodhouse et al., 2016a) to simulate the lahar's transit along the river channels from its starting  
562 location in the Eastern Cordillera to its end in the Sub-Andean zone, a distance of > 90 km and with a  
563 relief change of about 1500 m. Modeling results of LaharFlow, necessarily used the present  
564 topography, but shows strong similarity to deposit locations of the Mera lahar that we mapped in  
565 the field (Fig. 3 & 13), offers confirmation for the cross sectional areas of the lahar and also reaffirms  
566 the heights of the lahar terraces with a precision of  $\pm 10$  m. Output of the modeled lahar ceased to  
567 flow at Puyopungo, which is coherent with our final mapped point of the deposit. It is clear that since  
568 only scant Mera lahar deposits remain on the right margin of the Pastaza River, erosion on this bank  
569 has been preferential compared to the opposite margin where Mera lahar terraces are still found.  
570 Erosion has been preferential on this bank perhaps due to: 1) change of position of the Pastaza River  
571 channel (Burgos, 2006; Bernal et al., 2012), 2) effects of younger volcanism from the Madre Tierra  
572 (Calcaurco) volcanoes (Ball, 2015) or by action of reverse fault systems (Mirador, Bobonaza) that could  
573 have covered or remobilized the deposit or changed the river's course. Furthermore, at its farthest  
574 mapped extent the Mera lahar deposit underwent burial by a DAD from Sangay volcano at about 29  
575 ka (Valverde et al., 2015).

576

## 577 **7.1 CONCLUSIONS**

578

579 The Mera deposit is a secondary lahar deposit borne as a result of the transformation of a debris  
580 avalanche breccia that mixed with water and debris after rupture of an impounded temporary  
581 reservoir then flowed down the Pastaza River. The DAD of Huisla volcano is the best candidate as the  
582 source for the mainly monolithologic matrix and clasts comprising the Mera lahar.

583

584 The debris avalanche was produced by a sector collapse of the central peak/dome of Huisla volcano  
585 which slid into the Patate River valley. Radially fractured bombs found in the avalanche breccias on  
586 Huisla's northeast slopes, also in the Mera lahar deposit, and a fall deposit of fresh lithic clasts lying

587 between the two avalanche layers, suggests that the volcano was active at the time of collapse.  
588 Another possible factor contributing to the collapse is strike-slip movement of the transpressive  
589 fault which cuts through the southern limb of Huisla volcano. Rupture of this fault was also cited  
590 as responsible for the destructive 1949  $M_w$  6.9 Pelileo earthquake (Beauval et al., 2013; Alvarado, et  
591 al., 2016). Earlier ruptures on the same fault were of similar magnitude or greater, such as the local  
592 04 February 1797 devastating Patate earthquake (Beauval et al., 2013).

593

ACCEPTED MANUSCRIPT

The Mera lahar is a matrix-rich but non-cohesive type (Scott and Vallance, 1995), with a matrix which is comprised of grain sizes smaller or equal to 2.0 mm (coarse sand size granules) that overall constitutes 60%, 40-70% and 50%, respectively of the proximal, central and distal categories of the samples. No clay or silt grain sizes were measured. The Mera lahar's sandy matrix on the whole did not support the transport of huge blocks (multiple meter diameter) far from source and its non-cohesiveness possibly permitted greater mixing with water, and thus also the formation of some minor fluvial stratigraphy, which is observed at the distal site of Santa Ana. Where the Mera deposit is last observed more than 90 km from source, the lahar had not transformed to a hyperconcentrated flow. At this distance clasts of 20-30 cm diameter are still observed suspended in the matrix. In most areas the lahar deposit has formed an important local morphology of isolated high stand terraces that are well preserved on the left margin of the Pastaza River. Output of the computational modeling program, LaharFlow, confirms the results of our mapping of the lahar's deposit and also the subsequent post-depositional erosion of the lahar.

Nonetheless, we have not confirmed in the field if the lahar actually covered the Tarqui –Nueva Vida swath, since erosion by river avulsions has been significant. The actual mapped area of the lahar represents a present volume of 1.2 km<sup>3</sup>. The modeled area gives a volume of 5.4 km<sup>3</sup> which is coherent with the input of 4 km<sup>3</sup> of DAD solids and 1.4 km<sup>3</sup> of water.



In areas of such high erosion and cloaking by jungle vegetation, modeling of the deposit is the only way to appreciate the lahar's full inundation zone. Without a doubt the channel conditions may have been very different in the late Pleistocene. Still at Moravia town, where the lahar has 70 meter thickness, it is possible to see the basal contact with rounded river cobbles. The Mera lahar left an exceptional identifiable deposit which is testimony to collapse of the central part of Huisla volcano, a little studied and only vaguely recognized volcano in the Eastern Cordillera of Ecuador. Although both Tungurahua and Carihuairazo volcanoes have had subsequent major eruptions and avalanches after the Huisla-Mera duo, their associated gravitational volcanoclastic flows have not overtopped the high-standing terraces or deposited upon the terrace surfaces left by the Mera lahar in the upper Amazon Sub-Andean zone, and therefore have been eroded and are not easy to identify. These important geomorphic remnants are testimony to the lasting footprints left by the late Pleistocene Mera lahar and which are still preserved in the Sub-Andean landscape. Given the widespread reach of the Mera lahar we are compelled to increase our knowledge about transformation from avalanche breccias that form temporary dams to lahar flows and to provide relevant information that steers society to be prepared for other potential major lahars, particularly at volcanoes which are sliced by an active fault.

## REFERENCES

- Alvarado, A., Audin, L. N., Lagreulet, S., Segovia, M., Font, Y., Lamarque, G.,

- Quidelleur, X. (2014). Active tectonics in Quito, Ecuador, assessed by geomorphological studies, GPS data, and crustal seismicity. *Tectonics*, 33, doi:10.1002/2012TC003224, 17.
- Alvarado, A., L. Audin, J. M. Nocquet, E. Jaillard, P. Mothes, P. Jarrín, M. Segovia, F. Rolandone, D. Cisneros (2016). Partitioning of oblique convergence in the northern Andes subduction zone: migration history and present-day boundary of the North Andean Sliver in Ecuador, *Tectonics*, 35 (5): 1048-1065.
  - Ball P., 2015 Geochemical analysis of Ecuadorian Back-Arc lavas. Department of Earth Sciences, St Hugh's College, University of Oxford, Candidate Number: 256975
  - Barragan R, Geist D, Hall ML, Larson P, Kurz M (1998) Subduction controls on the composition of lavas from the Ecuadorian Andes. *Earth Planet Sci Lett* 154:153–166
  - Beauval, C., Yepes, H., Palacios, P., Segovia, M., Alvarado, A., Font, Y., Aguilar, J., Troncoso, L., Vaca, S., 2013. An earthquake catalog for seismic hazard assessment in Ecuador. *Bull. Seismol. Soc. Am.* 103 (2A), 773–786. <http://dx.doi.org/10.1785/0120120270>.
  - Bernard, B., van Wyk de Vries, B., Barba, D., Leyrit, H., Robin, C., Alcaraz, S., & Samaniego, P. (2008). The Chimborazo sector collapse and debris avalanche: Deposit characteristics as evidence of emplacement mechanisms. *Journal of Volcanology and Geothermal Research*, 176, 36–43.
  - Bernal, C., Christophoul, F., & Soula, J. (2012). Gradual diversions of the Rio Pastaza in the Ecuadorian piedmont of the Andes from 1906 to 2008: role of tectonics, alluvial

fan aggradation, and ENSO events. *Int J Earth Sci (Geol Rundsch)*, Springer, 16.

- Bès de Berc, S., Baby, P., Soula, J., Rosero, J., Souris, M., Christophoul, F., & Vega, J. (2004). La superficie Mera-Upano: Marcador Geomorfológico de la incisión fluvial y del levantamiento tectónico de la Zona Subandina Ecuatoriana. *La Cuenca Oriente: Geología y Petroleo*, 153-167. [horizon.documentation.ird.fr/exl-doc/pleins\\_textes/doc34-08/010036207.pdf](http://horizon.documentation.ird.fr/exl-doc/pleins_textes/doc34-08/010036207.pdf)
- Burgos, J. (2006). Genese et progradation d'un cone alluvial au front d'une chaine active : exemple des Andes Equatoriennes au Neogene. These de Doctorat, Docteur de l'Université Paul Sabatier Toulouse III Spécialité : Sciences de la Terre et de l'Environnement,
- Bustillos, J. (2008). Las avalanchas de escombros en el sector del volcán Tungurahua. Tesis de Grado Inédita de Ingeniero Geólogo - EPN, 151. <http://bibdigital.epn.edu.ec/handle/15000/8682>.
- Capra L, Macías JL (2002). The cohesive Naranjo debris flow deposit (10 km<sup>3</sup>): a dam breakout flow derived from the Pleistocene debris-avalanche deposit of Nevado de Colima volcano (México). *Journal of Volcanology and Geothermal Research* 117: 213-235.
- Capra, L. (2006). Volcanic Natural Dams Associated With Sector Collapses: Textural And Sedimentological Constrains On Their Stability. *Italian Journal of Engineering Geology and Environment*, Special Issue 1, DOI: 10.4408/IJEGE.2006-01.S-22
- Champenois, J., Baize, S., Vallée, M., Jomard, H., Alvarado, A., Espin, P., Ekstrom,

- G. and Audin, L. (2017), Evidences of surface rupture associated with a low magnitude (Mw5.0) shallow earthquake in the Ecuadorian Andes. *J. Geophys. Res. Solid Earth*. Accepted Author Manuscript. doi:10.1002/2017JB013928.
- Clapperton, M. (1990). Glacial and volcanic geomorphology of the Chimborazo–Carihuairazo Massif, Ecuadorian Andes. *Transactions of the Royal Society of Edinburgh, Earth Sciences* 81, 91-116.
  - Crandell DR (1971) Postglacial lahars from Mount Rainier Volcano, Washington. *Geol Surv Prof Pap* 677: 1–73
  - Darnell, A., Phillips, J., Barclay, J., Herd, R., & Lovett, A. (2013). Developing a simplified geographical information system approach to dilute lahar modelling for rapid hazard assessment. *Bulletin of Volcanology*, 4 (713), 75.
  - Espín Bedón, P. (2014), Caracterización geológica y litológica de los depósitos laháricos de Mera, provincia de Pastaza. Tesis de Grado Inédita de Ingeniero Geólogo - EPN, 212. <http://bibdigital.epn.edu.ec/handle/15000/784>
  - Espín Bedón, P. A., Mothes, P. A., Hall, M. L., Bernal, C., & Valverde, V. (2015). The great lahar deposit «Mera» in the upper Amazon basin--formed by transformation of a volcanic avalanche in Ecuador's Sierra. Published in IUGG. 2015 General Assembly, Prague, Czech Republic.
  - Espín Bedón P., Almeida S., Mothes P., Andrade D., Vásconez F.J., Ramon P. (2017) Mapa Preliminar De Amenazas por Lahares Primarios Para La Zona Oriental Del Volcán Cayambe, VIII Jornadas de Ciencias de la Tierra, Quito-Ecuador
  - Fairchild, L. (1987). Quantitative analysis of lahar hazard. in Keller, S.A.H., ed.,

Mount St. Helens, five years after: Cheney, eastern Washington University Press.

- Hall, M., Robin, C., Beate, B., Mothes, P., & Monzier, M. (1999). Tungurahua Volcano, Ecuador: structure, eruptive history and hazards. *Journal of Volcanology and Geothermal Research* (91), 1–21.
- Hall M.L., Samaniego P., Le Pennec J.L., Johnson J.B. (2008), Ecuadorian Andes volcanism: A review of Late Pliocene to present activity, *Journal of Volcanology and Geothermal Research* 176 (2008) 1-6, doi:10.1016/j.jvolgeores.2008.06.012
- Hastenrath, S., 1981. *The Glaciation of the Ecuadorian Andes*. Balkema, Rotterdam, 159 pp.
- Heine K. (1994), *The Mera Site Revisited: Ice-Age Amazon In The Light Of New Evidence* *Quaternary International*, Vol. 21, pp. 113–119
- Herrera, F. (2013). *Caracterización de los depósitos de avalanchas de escombros en el tramo Píllaro-Patate*. Tesis de Grado, Universidad Central del Ecuador, 236. <http://www.dspace.uce.edu.ec/handle/25000/2750>.
- Hoffer, G., Eissen, J., Beate, B., Bourdon, E., Fornari, M., & Cotten, J. (2008). Geochemical and petrological constraints on rear-arc magma genesis processes in Ecuador: The Puyo cones and Mera lavas volcanic formations. *Journal of Volcanology and Geothermal Research*, 176, 107–118.
- Keen, H.F. (2015) *Past environmental change on the eastern Andean flank, Ecuador*. PhD Thesis, Department of Environment, Earth & Ecosystems, The Open University. <https://ecologyofthepast.info/2015/09/30/keen-phd-thesis-2015/>
- Le Pennec J-L, De Saulieu G., Samaniego P., Jaya D., Gailler L., (2013), A

Devastating Plinian Eruption At Tungurahua Volcano Reveals Formative Occupation at ~1100 cal BC in Central Ecuador. 21st International Radiocarbon Conference edited by A J T Jull & C Hatté, Vol 55, Nr 2–3, 2013, p 1199–1214.

- Lebras, M., Mégard, F., Dupuy, C., & Dostal, J. (1987). Geochemistry and tectonic setting of pre-collision Cretaceous and Paleogene volcanic rocks of Ecuador. *Geological Society of America Bulletin*, 99, 569-578.
- Lipman PW, Mullineaux DR (1981) The 1980 eruptions of Mount St. Helens, Washington. United States Geological Survey, Professional Paper, vol 1250, 844 pp.
- Liu, K., & Colinvaux, P. (1985). Forest changes in the Amazon Basin during the last glacial maximum. *Nature*, 318, 556-557.
- Loughlin, S.C., C. Vye-Brown, R.S.J. Sparks, S.K. Brown, and S. Jenkins, (2015). *Global Volcanic Hazards and Risk*. Cambridge, UK: Cambridge University Press. Available at <http://globalvolcanomodel.org/wp-content/uploads/2015/08/Global-Volcanic-Hazards-and-Risk-Full-book-low-res.pdf>.
- Manville, V. (2015). D. Rouwet et al. (eds.), *Volcanic Lakes*, *Advances in Volcanology*, DOI 10.1007/978-3-642-36833-2\_2, Springer-Verlag Berlin Heidelberg 2015
- Mothes, P., Hall, M. and Janda, R. (1998). The enormous Chillos valley lahar: an ash-flow-generated debris flow from Cotopaxi volcano, Ecuador. *Bulletin of Volcanology*, 59, 233-244.
- Mothes, P., Hall, M., Andrade, D., Samaniego, P., Pierson, T., Ruiz, G., & Yepes, H. (2004). Character, Stratigraphy and Magnitude of historical lahars of

Cotopaxi Volcano (Ecuador). *Acta Vulcanologica*, 16 (1-2), 85-108.

- Mothes P. and Hall M., (2008). Rhyolitic calderas and centers clustered within the active andesitic belt of Ecuador's Eastern Cordillera, COLLAPSE CALDERAS WORKSHOP 19–25 October 2008, Querétaro, Mexico, Extended abstract: <http://herald.iop.org/EESvol13/m97/hxp//link/2062>
- Mothes, P., Vallance, J. (2015). Lahars at Cotopaxi and Tungurahua Volcanoes, Ecuador: Highlights from Stratigraphy and Observational Records and Related Downstream Hazards. In: *Volcanic Hazards, Risks, and Disasters*. Elsevier, pp. 141-168.
- Pierson, T.C., Wood, N.J. & Driedger, C.L. Reducing risk from lahar hazards: concepts, case studies, and roles for scientists. *J Appl. Volcanol.* (2014) 3: 16. <https://doi.org/10.1186/s13617-014-0016-4>
- Pierson, T., & Scott, K. (2014). Hydrogeomorphic Effects of Explosive Volcanic Eruptions Drainage Basins. *Annu. Rev. Earth Planet. Sci.*, 469–507.
- Pratt, W., Duque, P., & Poncec, M. (2005). An autochthonous geological model for the eastern Andes of Ecuador. *Tectonophysics*, 399, 251-278.
- Peccerillo, A., & Taylor, S. (1976). Geochemistry of eocene calc-alkaline volcanic rocks from the Kastamonu area, northern Turkey. *Contributions to Mineralogy and Petrology*, 58, 63-81.
- Pouliquen O. (1999), Scaling laws in granular flows down rough inclined planes, *Physics of Fluids* 11, 542 (1999); doi: <http://dx.doi.org/10.1063/1.869928>.

- Reid, ME, Sisson TW, and Diane L. Brien. Volcano collapse promoted by hydrothermal alteration and edifice shape, Mount Rainier, Washington. (2001). *Geology*; September; v. 29; no. 9; p. 779–782
- Samaniego, P., Barba, D., Robin, C., Fornari, M., & Bernard, B. (2012). Eruptive history of Chimborazo volcano (Ecuador): A large, ice-capped and hazardous compound volcano in the Northern Andes. *Journal of Volcanology and Geothermal Research* 221–222, 33-51.
- Schiano, P., Monzier, M., Eissen, J., Martin, H., & Koga, K. (2010). Simple mixing as the major control of the evolution of volcanic suites in the Ecuadorian Andes. *Contrib Mineral Petrol*, 160, 297 – 312.
- Scott, K.M., and Vallance, J.W., 1995, Debris flow, debris avalanche, and flood hazards at and downstream from Mount Rainier, Washington: U.S. Geological Survey Hydrologic Investigations Atlas 729, 2 sheets, 9 p.
- Scott, K., & Vallance, J.W and Pringle, P. T (1995). Sedimentology, behavior, and hazards of debris flows at Mount Rainier, Washington. U.S. Geological Survey Professional Paper, 1547, 56.  
  
Scott, K.M. and Vallance, J.W (1995), Sedimentology, behavior, and hazards of debris flows at Mount Rainier, Washington: U.S. Geological Survey Professional Paper 1547, 56 p.
- Vallance, J. (2000). Lahars. En H. Sigurdsson (Ed.), *Encyclopedia of Volcanoes* (págs. 601-616). USA: Academic Press.
- Vallance, J.W., Iverson, R. (2015). Lahars and their deposits. In: Sigurdsson, H.,



Houghton, B.F., McNutt, S.R., Rymer, H., Stix, J. (Eds.), Encyclopedia of Volcanoes. Academic Press, London, pp. 649-664.

- Valverde, V. (2014). Las avalanchas de escombros provenientes del volcán Sangay: caracterización petrográfica-geoquímica. Tesis de Grado Inédita de Ingeniero Geólogo - EPN, Quito, No. 151.
- Vásconez, R., Hall, M., & Mothes, P. (2011). Devastadores flujos de lodo disparados en el volcán Carihuayrazo por el terremoto del 20 de Junio de 1698. Revista Politécnica: Monografía de Geología 7, 30(1), 86-105.
- Woodhouse M.J., Bates P.B., Hogg A.J., Phillips J.C. & Rougier J.C. (2016), Topographic uncertainty in models of geological hazards: a general statistical framework and application to a lahar hazard model using SRTM elevation data. Cities on Volcanoes 9. Puerto Varas Chile.
- Woodhouse M.J., Johnson C.G., Hogg A.J., Phillips J.C., Espín Bedón P.A., Almeida S., Andrade D. (2016), LaharFlow: a web-based lahar hazard model. Cities on Volcanoes 9. Puerto Varas Chile.

**Highlights of the Mera Lahar study:**

-Detailed petrographic fingerprinting shows that Huisla volcano's DAD breccias provided the bulk clastic material to form the Mera lahar.

-Huisla volcano had a late Pleistocene collapse, possibly from shaking provoked by the transpressive active fault under its SW shoulder. Eruptive activity is also suspect, due to finding radially fractured bombs in both the Huisla DAD deposit and the Mera lahar.

-Temporary dams formed from the DAD blockage in deep canyons and impounded the river system. Once the dams ruptured the ensuing mixture of water and breccia formed an enormous secondary lahar (volume  $\sim 5 \text{ km}^3$ ) that flowed to the Sub-Andean-western Amazon area, some 90 km from source. Passage was along the channel of the master Pastaza river.

-The lahar deposit is characteristically rich in the Huisla DAD breccias, has a high sand grain content, was a non-cohesive type and did not transform to a hyperconcentrated flow.

-The deposit is still well preserved on the left margin of the Pastaza river, where 30-50 m high terraces now host the towns of Mera and Shell, among others.

-Mapping was complex due to jungle vegetation and erosion caused by avulsions of the Pastaza river.

-The modeling program LaharFlow provided results that show good similarity with the field mapping in certain preserved areas, ie Mera and Shell and also showed where the deposit may have been, but which we now find no evidence, since erosion or burial has been very complete.

-A log was extracted from Mera lahar's interior and a radio carbon date of  $> 43.5 \text{ ka}$  was obtained. Overlying dated strata (17 ka - 40.5 ka) provide minimum ages for the Mera lahar.

-Due to its long distance lahar, the low profile volcano Huisla with its collapse events provoked a major lahar, whose deposits are clearly recognizable some 40 ka after the event.